frontiers | Frontiers in Marine Science

ORIGINAL RESEARCH
published: 06 May 2022
doi: 10.3389/fmars.2022.860910

An Eco-Morphodynamic Modelling Approach to Estuarine Hydrodynamics & Wetlands in Response to Sea-Level Rise

Kristian Kumbier[1], Kerrylee Rogers[1], Michael G. Hughes[2], Kirti K. Lal[2], Laura A. Mogensen[1] and Colin D. Woodroffe[1]*

[1] School of Earth Atmospheric and Life Sciences, University of Wollongong, Wollongong, NSW, Australia, [2] Science, Economics and Insights Division, NSW Department of Planning, Industry and Environment, Sydney, NSW, Australia

OPEN ACCESS

Edited by:
Zeng Zhou,
Hohai University, China

Reviewed by:
Mark Schuerch,
University of Lincoln, United Kingdom
A. Rita Carrasco,
University of Algarve, Portugal
Jean-Philippe Belliard,
University of Antwerp, Belgium

***Correspondence:**
Kristian Kumbier
kak609@uowmail.edu.au

Specialty section:
This article was submitted to Coastal Ocean Processes, a section of the journal Frontiers in Marine Science

Received: *24 January 2022*
Accepted: *01 April 2022*
Published: *06 May 2022*

Citation:
Kumbier K, Rogers K, Hughes MG, Lal KK, Mogensen LA and Woodroffe CD (2022) An Eco-Morphodynamic Modelling Approach to Estuarine Hydrodynamics & Wetlands in Response to Sea-Level Rise. Front. Mar. Sci. 9:860910. doi: 10.3389/fmars.2022.860910

Tidal inundation is the primary driver of intertidal wetland functioning and will be affected by sea- level rise (SLR). The morphology of estuaries and friction across intertidal surfaces influences tidal propagation; accordingly, sea-level rise not only increases inundation frequency, but will also alter other tidal parameters, such as tidal range. To investigate responses of estuarine intertidal vegetation, primarily mangrove and saltmarsh, to SLR an eco-morphodynamic modelling approach was developed that accounted for some of the feedbacks between tidal inundation and changes to wetland substrate elevations. This model partially accounts for adjustment in estuarine hydrodynamics, and was used to examine the potential effect of SLR on mangrove and saltmarsh distribution in a micro-tidal channelised infilled barrier estuary in southeast Australia. The modelling approach combines a depth-averaged hydrodynamic model (Telemac2D) and an empirical wetland elevation model (WEM) that were coupled dynamically to allow for eco-geomorphological feedbacks. The integrated model was parameterised to consider two SLR scenarios, and two accretion scenarios within the WEM. Time series of observed water levels, tidal inundation and flow velocity were used to validate the hydrodynamic model for present-day sea level, whereas wetland mapping was used to verify predictions of mangrove and saltmarsh distribution. Tidal range varied along the estuary, increasing in response to low and high SLR scenarios (by up to 8%), and responded non-linearly under high SLR. Simulations of low and high SLR scenarios indicated that wetlands mostly withstand modest SLR rates (+ 5mm yr^{-1}) through sedimentation, but submerge and convert to subtidal areas under fast SLR rates (> 10mm yr^{-1}). Projected changes in tidal range are linked to eco-geomorphological feedbacks caused by changing wetland extents and adjustments of intertidal wetland geomorphology through sedimentation. Potential changes arising from morphological change at the entrance and in the tidal channels is not obtained from the model. The results of this study demonstrate

interconnections between hydrodynamics and intertidal wetlands, which need to be accounted for when estimating wetland response to SLR in channelised estuaries. Integrated models of estuarine-wetland systems are more precise as they account for the dynamic feedbacks between hydrodynamics and wetlands. For example, they also consider alterations to tidal range resulting from SLR and the effects of these on wetland inundation and sedimentation.

Keywords: hydrodynamic modelling, Telemac2D, mangrove, saltmarsh, hydroperiod, Australia

1 INTRODUCTION

Intertidal wetlands, comprising mangroves and/or saltmarsh, are among the most productive ecosystems in the world, providing ecosystem services to coastal communities, such as coastal protection, erosion control, maintenance of fisheries, and opportunities to mitigate climate change through carbon sequestration (Barbier et al., 2011; Gedan et al., 2011; Rogers et al., 2019a). Low-energy coastal environments within deltas and estuaries that are regularly inundated by tidal water provide the shelter intertidal wetlands require to develop (Woodroffe et al., 2016). Many studies suggest that tidal dynamics control halophytic species distribution through variation in characteristics of wetland inundation regime, such as inundation duration or frequency (Watson, 1928; Baltzer, 1969; Spier et al., 2016; Kumbier et al., 2021). Sea-level rise (SLR), as projected by the Intergovernmental Panel on Climate Change (IPCC) and others (Church et al., 2013; Dangendorf et al., 2017), will change the tidal regime and alter relationships between sedimentation and wetland elevation (Allen, 2000; McKee et al., 2012). This may cause wetlands to respond through a combination of landward migration and vertical adjustment, which both depend on the rate of SLR (Woodroffe, 2018). Eco-geomorphological feedbacks serve to maintain coastal wetland substrates *in situ* by facilitating vertical growth when the sea is rising (Kirwan et al., 2010; McKee et al., 2012).

Many empirical and physical studies involving hydrodynamic modelling have investigated the response of tidal wetlands to SLR (e.g. Morris et al., 2002; Craft et al., 2009; Alizad et al., 2016a). Numerical models of physical processes resolve water and sediment flows across the wetland based on simplified hydrodynamic schemes, whilst empirical models use statistical relationships derived from observations of spatial sedimentation patterns, below-ground processes, and tidal inundation (Fagherazzi et al., 2012).

The geomorphological evolution of intertidal wetlands involves feedbacks between wetland inundation regime and sedimentation, which manifests in a development from low to high elevated wetlands. This evolution is driven by initially prolonged tidal inundation and high sedimentation that gradually decrease in time with increasing surface elevation (e.g. potentially leading to mangroves being replaced by saltmarsh). However, these natural dynamics are modified by SLR. Wetland vegetation zonation arises in response to inundation regimes, and a change to these inundation regimes (e.g. by SLR) will result in changes to the vertical distribution of wetlands, which is reflected in recent observations of mangrove encroachment into saltmarsh in southeast Australian estuaries (e.g. Saintilan et al., 2014). Within estuaries, changes in wetland inundation regime are not only driven by SLR itself (e.g. an increase in mean water level) but also by alteration of the overall hydrodynamics of the estuarine system, such as increasing tidal range in response to SLR (Lee et al., 2017; Du et al., 2018; Kumbier et al., 2018a). However, changes in estuarine hydrodynamics are rarely considered in assessments of wetland response to SLR, despite research indicating interconnections between the two and suggestions that wetland modelling in estuaries may have to account for tidal modifications (Mogensen and Rogers, 2018). This most likely relates to the challenges of coupling computationally demanding hydrodynamic models with empirical models of wetland evolution, but may cause imprecise estimates of wetland response to SLR in complex estuarine environments where tidal dynamics change under SLR.

Empirical models of wetland change with SLR aim to account for and quantify biophysical processes involved in the evolution of wetlands, such as trapping of mineral sediment, organic sedimentation through vegetation growth, or soil compaction (Cahoon et al., 2006; Cahoon et al., 2011; Krauss et al., 2014). Model inputs commonly include field measurements of surface elevation change using techniques such as the surface elevation table (SET) approach (Morris et al., 2002; Oliver et al., 2012; Rogers et al., 2012), suspended sediment concentrations (Temmerman et al., 2003a; Temmerman et al., 2003b) and dating of sediment cores for accretion rates (Mudd et al., 2009; Thorne et al., 2018). Such empirical data on sedimentation has been combined with tidal measurements (e.g. depth below high tide) to estimate the evolution of wetlands, with studies suggesting either linear or exponential relationships between inundation (or elevation used as a proxy for inundation) and mineral sedimentation (Krone, 1987; Cahoon and Reed, 1995; Temmerman et al., 2003b). However, relationships between tidal inundation and sedimentation may differ between sites due to the complex multidimensional interconnection of geomorphology, hydrodynamics, and ecology in tidal wetlands. In consequence, empirical models of wetland evolution developed for one study site may have limited applicability to other sites (Mogensen and Rogers, 2018; Wiberg et al., 2020; Rogers and Saintilan, 2021), which is particularly true for highly parameterised, site-specific models. Overall, empirical modelling studies as outlined above

contribute to process understanding of wetland evolution, and can be used to estimate wetland responses to SLR (e.g. Morris et al., 2002; Craft et al., 2009); however, the complex field data collection associated with the development and parameterisation of such models has restricted most studies to individual wetland sites rather than entire estuarine systems. A limitation of locally focused studies is the representation of tidal hydrodynamics and wetland inundation regimes, which are generally inferred from a few tide gauges in the vicinity of the study site, with tidal range assumed to remain unaffected by SLR (Morris et al., 2002; Rogers et al., 2012; Thorne et al., 2018). Furthermore, inferring wetland inundation regimes from a calculation of tide gauge data and surface elevation neglects the drag wetland vegetation can exert on tidal flow (Temmerman et al., 2005). In addition, tidal regimes inside estuaries have been shown to alter under SLR (Lee et al., 2017; Du et al., 2018; Kumbier et al., 2018a), which may affect wetland sedimentation as, for example, inundation durations can increase and so may mineral sediment supplied to a wetland (Temmerman et al., 2003a).

Numerical modelling studies of physical processes driving wetland response to SLR involving hydrodynamic modelling can resolve limitations regarding alteration of hydrodynamics (e.g. tidal regime) and representation of wetland inundation regimes if applied at the scale of an entire estuary; however, most studies combining hydrodynamic and wetland evolution models have been restricted to small study sites (e.g. D'Alpaos et al., 2007; Temmerman et al., 2007; Rodríguez et al., 2017), and thus, responses in estuarine hydrodynamics could not be represented properly. This limitation is likely related to research objectives focusing on processes operating over small scales, and the high computational demands of modelling at the scale of an estuary. Only a few numerical modelling studies estimated wetland response to SLR at the scale of an estuary whilst accounting for hydrodynamic system responses (Hagen et al., 2013; Alizad et al., 2016a; Alizad et al., 2016b; Alizad et al., 2018). For example, a two-dimensional hydrodynamic model has been coupled with a zero-dimensional marsh model to assess the response of saltmarsh to SLR in the lower St. Johns River in northern Florida, USA. Utilising a hydrodynamic model (ADCIRC), Hagen et al. (2013) extended the Morris et al. (2002) zero-dimensional empirical wetland model for saltmarsh productivity and surface elevation change, to develop a coupled two-dimensional model that accounts for alteration of hydrodynamics. The hydrodynamic modelling component thereby provided generalised tidal levels (e.g. Mean High Water [MHW]), which were then included as inputs into the Morris et al. (2002) wetland model to calculate biomass productivity, vertical accretion rates and surface elevation change under different SLR scenarios. This eco-hydraulic model has been further refined for the same study site to include bio-physical feedback through a time-stepping framework which facilitates stepwise increases in wetland surface elevation and adjustment of bottom friction coefficients at defined intervals (Alizad et al., 2016a), as well as consideration of river discharge for fluvial estuarine systems (Alizad et al., 2016b).

Coupled eco-hydraulic models as outlined above allow for an assessment of wetland response to SLR whilst accounting for system responses in hydrodynamics; however, the applicability of this particular model (Alizad et al., 2016a; Alizad et al., 2016b; Alizad et al., 2018) may be limited only to *Spartina* saltmarsh sites through North and South America (and similar settings) due to the coupling with Morris et al.'s (2002) model, which was specifically developed for low elevated saltmarshes in the US which are characterised by low biodiversity (e.g. *Spartina* only) and decomposition rates that are well balanced against additions. However, many wetlands are more complex, with more zonation and vegetation diversity, which may limit the model's application in complex wetlands comprising co-existing mangrove and high saltmarsh, such as found in southeast Australia where decomposition and autocompaction has been shown to be particularly important (Rogers and Saintilan, 2021). Furthermore, coupled hydrodynamic-wetland models may be improved through spatially explicit consideration of wetland inundation regimes rather than generalised tidal levels (e.g. MHW), as the latter have been shown to represent wetland zonation patterns only at the broadest level (Kumbier et al., 2021). Such modelling of spatially explicit wetland inundation regimes (e.g. inundation duration) would also allow for consideration of floodplain flow attenuation (Temmerman et al., 2005).

This study presents a coupled eco-morphodynamic modelling approach utilising a depth-averaged hydrodynamic model (Telemac2D) and an empirical wetland elevation model developed for this study (WEM). The two-way coupled model accounts for responses in estuarine hydrodynamics caused by SLR, as well as alteration in hydrodynamics due to eco-geomorphological feedbacks on the wetland only (e.g. surface elevation changes). Thereby, the distribution of mangrove and saltmarsh in response to SLR is estimated through a spatially explicit calculation of wetland inundation regime (e.g. average inundation duration). Changes in wetland surface elevation are implemented using two empirical relationships (slow and moderate growth) between simulated wetland inundation regime and observations of changes in wetland surface elevation derived from a 20-year observational record. Low and high SLR scenarios have been simulated to investigate responses of mangrove and saltmarsh to increased inundation in a micro-tidal infilled barrier estuary in southeast Australia. Whereas components of the coupled eco-morhodynamic model were specifically developed and parameterised for the study site (e.g. WEMs), it was an overall aim to present a transferable modelling framework with respect to the technical aspects of coupling estuarine hydrodynamics and intertidal wetlands.

The objectives of this study were to:

1. develop a transferable eco-morphodynamic modelling framework by coupling a hydrodynamic model and an empirical wetland elevation model; and
2. estimate changes in mangrove/saltmarsh distribution in response to SLR at the scale of an entire estuary, as well as changes in system hydrodynamics relevant for wetland modelling.

Improved understanding of interconnections between hydrodynamics and wetlands under SLR can support planning and decision making for estuarine-wetland systems, which are at present typically studied in separation.

2 MATERIALS AND METHODS

2.1 Study Site

Minnamurra River estuary is located on the wave-dominated southeastern coast of NSW, Australia. The estuarine system is classified as a wave-dominated barrier estuary (Roy et al., 2001), and tides are the dominant source of hydrodynamic energy within the estuary. Hydrodynamics inside the estuary are only affected by river discharge during and following large rainfall events (Ryan, 1992), with tides being semi-diurnal and displaying a significant diurnal inequality. The open ocean tide range reaches a maximum of approximately 2 m during spring tides, but is attenuated at the estuary's entrance during spring tide conditions by approximately 20%, and is comparatively constant throughout the lower 7 km of the estuary, except for minor tidal amplification of a few centimetres occurring where the main channel narrows (Kumbier et al., in review). The estuary has a catchment of approximately 142 km^2, with Rocklow Creek being the largest tributary (24 km^2). A well-defined main channel, which is partly surrounded by low-lying intertidal areas where mangrove and saltmarsh occur (**Figure 1**), evolved as a result of sedimentary infilling in the past 8000 years (Panayotou et al., 2007; Haslett et al., 2010). Elevations in **Figure 1** are given in metres relative to Australian Height Datum (AHD), with mean sea level inside the estuary now positioned at approximately 0.1 m AHD due to rising sea-level since the datum's establishment in 1968, and the temporary increases in mean water level during spring tides when tidal pumping elevates mean water level.

Intertidal wetlands of mangrove and saltmarsh occur in the upper half of the tidal frame, and have been mapped broadly by Chafer (1998) and in more detail by Owers et al. (2016). A detailed analysis of wetland inundation regimes for these mangrove and saltmarsh communities has been presented by Kumbier et al. (2021). Accordingly, *Avicennia marina* occupy intertidal areas with a total inundation duration of approximately 30-75% of the time, at a frequency of 1.5-2 inundations per day, and for an average duration of 2.7-5 hours per event. An ecotone with a combination of *Avicennia marina* mangroves and dense shrubby *Aegiceras corniculatum* mangroves occurs where the total inundation duration is approximately 15-30%, the daily inundation frequency between 0.9-1.5, and the average inundation duration 2-2.7 hours per event. Higher in the tidal frame (approximately from an elevation of 0.55 m AHD), saltmarsh species such as *Sporobolus virginicus*, *Sarcocornia quinqueflora* and *Juncus krausii* occupy elevations being subject to total inundation duration of <15%, inundation frequencies below 0.9 tides per day, and average inundation duration of 0.85-2 hours per event. *Casuarina glauca* forest border saltmarsh in supratidal positions on the floodplain. Mangroves, saltmarsh and *Casuarina* follow a distinct zonation across the floodplain, but the encroachment of mangroves into saltmarsh, as well as saltmarsh beneath *Casuarina*, associated with contemporary SLR in recent

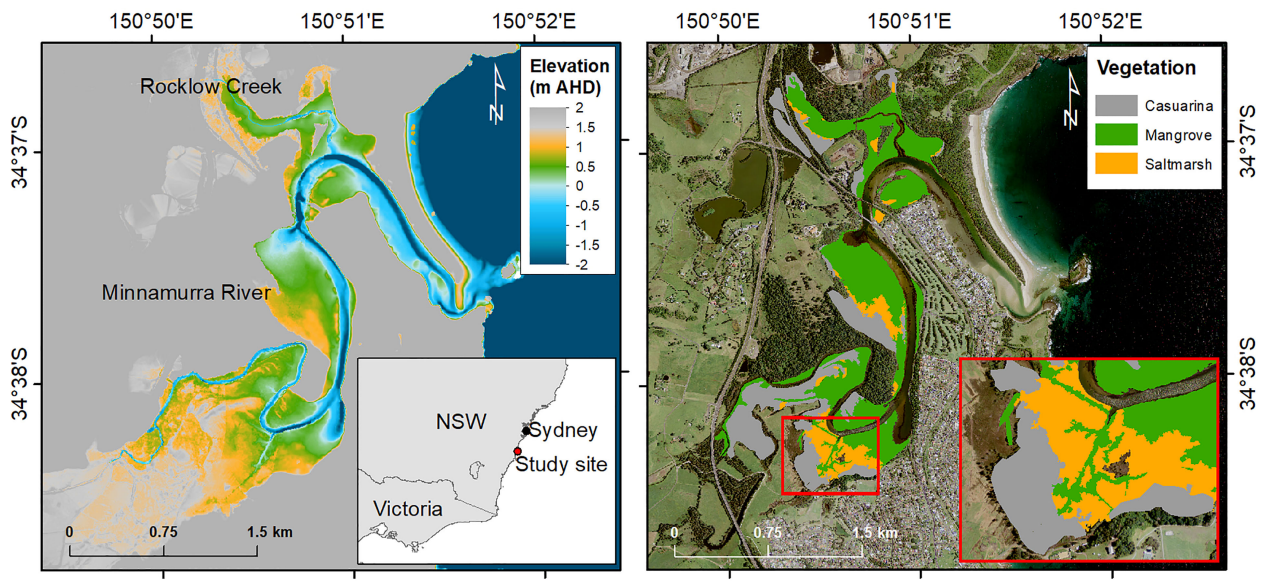

FIGURE 1 | Bathymetry and topography of Minnamurra River estuary (left), and intertidal wetland vegetation communities (right). Lidar-derived topography and sonar-derived bathymetry sourced from Geoscience Australia (2018; 2011), Department of Planning Industry and Environment (2017) and University of New South Wales (2017). Wetland mapping adjusted from Owers et al. (2016) and Chafer (1998).

decades may at times obscure these patterns (Chafer, 1998; Saintilan et al., 2018).

2.2 Methods

2.2.1 Overall Model Description

The coupled eco-morphodynamic model consists of two main components, a hydrodynamic model and an empirical wetland elevation model (WEM) (**Figure 2**). Tidal conditions under SLR at Minnamurra River estuary were simulated utilising the hydrodynamic model Telemac2D (more details in section 2.2.2). Mean sea level was increased incrementally at 10-year intervals and model outputs of each tidal simulation (length of 28 days) were processed into maps of average inundation duration. These maps were imported into ArcGIS to project intertidal wetland vegetation zonation (mangrove and saltmarsh). Changes in wetland surface elevation were determined using two linear relationships (slow and moderate vertical growth) between modelled average inundation duration and observations of surface elevation changes in mangrove and saltmarsh from the past 20 years (2001 – 2021). Updates of wetland topography and bottom friction in response to SLR were implemented utilising the pre-/post-processing software BlueKenue®, and subsequently used in the hydrodynamic model for the next iteration. The coupling time step between the hydrodynamic and wetland model was set to 10 years, and thus allows for eco-geomorphological feedback exchange between estuarine hydrodynamics and intertidal wetlands every 10 years.

2.2.2 Hydrodynamic Model

The hydrodynamic model Telemac2D solves the depth-averaged Saint-Venant shallow water equations in two dimensions and thus accounts for processes such as continuity and momentum transfer (Hervouet, 2000). The model has been demonstrated to be suitable for simulating estuarine hydrodynamics (Seenath et al., 2016; Stark et al., 2017; Iglesias et al., 2019). In this study the model was set up using a finite element method solver for numerical discretization of the shallow water equations on an unstructured triangular mesh grid, which provided the flexibility required for modelling hydrodynamics in complex environments with varying channel width, as occurs at Minnamurra River estuary (**Figure 3**). For a full description of the equations solved by Telemac2D, refer to Hervouet (2007) and the software user manual (Telemac2D, 2014).

The graphical user interface BlueKenue® was used to create a triangular mesh grid with varying mesh sizes in order to resolve the hydrodynamics observed in the field. Larger mesh elements of 15-65 m size were created offshore, whereas the narrow entrance channel was refined to a mesh element size of 5 m length. A mesh size of 5 m was also chosen along the thalweg of the river, which was refined to 3 m in the most upstream locations due to the narrowing of the main channel. Intertidal areas were represented with mesh elements of 10 m length, which resulted in an overall triangular mesh grid with 86563 nodes and 170094 elements (**Figure 3**). Parallel computation was used to overcome the computational demands caused by a large and detailed modelling domain. An open boundary for tidal forcing was defined along the eastern margin of the model domain that was driven by a time-series of water level data collected at the Jervis Bay tide gauge located approximately 50 km south of the study site. It was assumed that the Jervis Bay tidal data was representative of open coast tidal conditions offshore of Minnamurra River estuary. The model did not consider short-period waves as these have been shown to only affect water levels in the entrance channel (Kumbier et al., 2022).

Particular care was taken to ensure the correct representation of topography and bathymetry in the study area. Accordingly, a seamless topo-bathymetric digital elevation model (DEM) was developed, which included a combination of three LiDAR data sets (Geoscience Australia, 2011; University of New South Wales, 2017; Geoscience Australia, 2018), as well as single beam

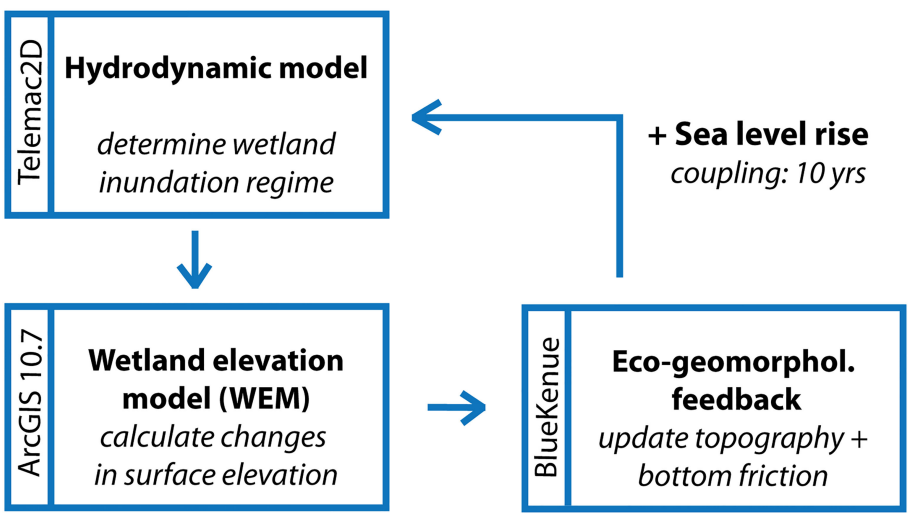

FIGURE 2 | Schematic illustration of the coupled hydrodynamic-wetland modelling framework.

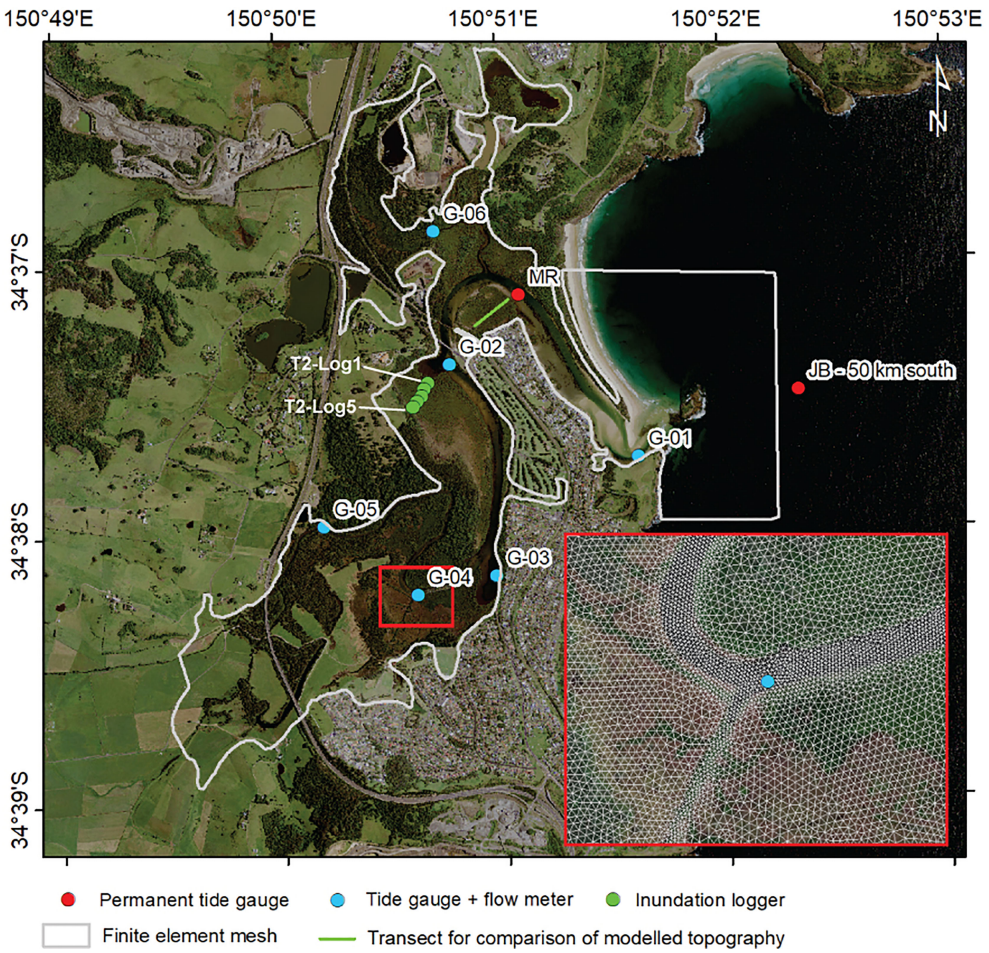

FIGURE 3 | Telemac2D finite element mesh model and location of tidal observations used for calibration and validation procedures. The grey polygon shows the extent of the Telemac2D model whereas the red box presents an example of the mesh-grid layout. The green transect indicates where modelled changes in wetland topography have been compared.

bathymetry data (OEH, 2017). As intertidal areas surrounding Rocklow Creek were found to be poorly represented, 350 real time kinematics-global positioning system (RTK-GPS) elevation measurements were collected (vertical accuracy of 1.5 cm), to correct the DEM. Since inundation modelling and assessing wetland response to SLR is particularly sensitive to topographic inputs (Mogensen and Rogers, 2018; Alizad et al., 2020), the quality of the seamless topo-bathymetric DEM was investigated by comparison with 1128 RTK-GPS elevation measurements taken in mangrove and saltmarsh areas across the estuary. These RTK-GPS points were not used in the creation of the seamless DEM and were only used to verify the quality of the seamless DEM; a high coefficient of determination of 0.89 and RMSE of 0.07 m with no spatially distributed biases provided support that the seamless DEM was a reasonable representation of intertidal wetland topography (**Supplementary S1**).

Spatially varying bottom roughness with regard to land-use types and wetland vegetation communities was defined using Manning's friction coefficients taken from the literature (Chow, 1959; Arcement and Schneider, 1989; Kaiser et al., 2011). Accordingly, open water and channels were represented with a value of 0.02, mangroves with a value of 0.035, saltmarsh with a value of 0.05 and *Casuarina* forest with a friction coefficient of 0.1.

The hydrodynamic model was calibrated and validated following commonly applied procedures of using separate time periods for model calibration and validation (Williams and Esteves, 2017). The model calibration was undertaken by comparison of modelled and observed water levels and wetland inundation depths from 23 November 2019 to 26 November 2019. This relatively short time-period allowed for repeated model runs to iteratively calibrate the model by varying mesh element sizes in critical locations (e.g. refinement in narrow channel sections to prevent tidal energy dissipation) and testing different bottom friction coefficients in the main channel and intertidal areas. A spin-up period of 1 day was found to be reasonable to dissipate the effects of initial conditions inside the model domain.

Validation of the model was based on comparison of observed and modelled water levels, flow velocities and inundation depths for an extended time period covering spring and neap tide conditions between 27 November and 10 December 2019. This validation was undertaken for various locations along the estuary (see **Figure 3**) and considered tidal gauge data from one permanent tide gauge (MR) and water-level time-series data from pressure transducers (G-01 to G-06), tidal velocity measurements using an acoustic Doppler current profiler (ADCP) near the permanent tide gauge (MR), tidal velocity measurement using drag-tilt flow meters (JCU Geophysics Laboratory, 2020), as well as wetland inundation logger data. The quality of water-level outputs of the hydrodynamic model was calculated using correlation coefficients and RMSE following Kumbier et al. (2018b).

SLR scenarios of 0.4 m (RCP2.6) and 0.9 m (RCP8.5) by 2100 (relative to 1986-2005) were selected to represent the lower and upper boundary of the IPCC's AR5 SLR projections and estimates for the Australian coastline (Church et al., 2013; McInnes et al., 2015; Zhang et al., 2017). These two scenarios were selected to investigate the response of wetlands to slow and fast rates of SLR. Mean sea level was increased from 2020 incrementally every 10 years in a linear manner for the lower RCP2.6 (+ 5 mm yr^{-1}) and an exponential manner for the higher RCP8.5 (+ 7-14 mm yr^{-1}) SLR scenario (**Supplementary S2**) as reported by Church et al. (2013). These increases in mean sea level were added to time-series of water level from the open ocean tide gauge in Jervis Bay, and the model was run for one lunar tidal cycle (28 days) to account for water-level variations during the spring-neap cycle. River discharge was not included in the model because spatial distribution of wetland vegetation in this estuary is largely a function of tidal inundation regime (Kumbier et al., 2021), only negligible discharge was recorded during the calibration data collection due to low flow conditions, and field observations indicated that the estuary's hydrodynamics are primarily driven by tides and only affected by discharge during larger rainfall events (Ryan, 1992).

Water-level outputs from tidal simulations were further investigated for changes in spring tidal range at monitoring locations shown in **Figure 3**. Peaks and troughs were extracted to determine differences between consecutive high and low waters, and to ultimately determine the maximum modelled tidal range under SLR at a particular location.

2.2.3 Empirical Wetland Elevation Model

2.2.3.1 Wetland Inundation Regime

Outputs of intertidal water depths from the hydrodynamic model were converted at each 10-year coupling time step to raster data of average inundation duration per inundation event. Therefore, Benson's (2020) Matlab code for processing of Telemac2D files was extended to iterate through all output time steps (every 5 min * 28 days = 40320 time steps) and mesh elements (170094), to determine average inundation durations per event at each mesh element. In particular, the average inundation duration was determined by identification of all high water inundation peaks and their respective duration exceeding a threshold of 0.01 m water depth, and averaging these durations for all inundation peaks. These spatially explicit estimates of average inundation duration per event were then used to determine the distribution of mangrove and saltmarsh based on site-specific empirical inundation observation reported in Kumbier et al. (2021). Accordingly, areas with an average inundation duration greater than 5 hours per inundation event were assumed to be low-elevation tidal flats or river channel, areas with a duration between 2-5 hours were assumed to be mangroves, whereas areas with a duration of between 0.85-2 hours were assumed to be saltmarsh. No separation between *Avicennia marina* and *Aegiceras corniculatum* mangroves was made because of overlap in their distribution and limited knowledge on sedimentation and inundation dynamics of *Aegiceras corniculatum* (Kumbier et al., 2021). Supratidal *Casuarina* wetlands were not included in the model because too little is known on their preferred tidal inundation regime.

2.2.3.2 Wetland Model Parameterisation

Empirical data on wetland surface elevation change was extracted from a 20-year data series of surface elevation change observed using a network of three SETs in the mangrove zone and three SETs in the saltmarsh zone between 2001 and 2021 (**Supplementary S3**). SETs serve as a benchmark against which changes in wetland surface elevation can be determined over time and the technique has been described by Cahoon et al. (2002) and previously reported for this site (Oliver et al., 2012; Rogers et al., 2012; Lal, 2019).

The WEM developed for this study considered vertical changes in surface elevation beneath mangrove and saltmarsh through a linear relationship between the average rates of elevation gain of mangrove/saltmarsh over the 20 year monitoring period and simulated average inundation duration. Most studies relate wetland surface elevation change and tidal inundation using either a linear or exponential model structure (Cahoon and Reed, 1995; Morris et al., 2002; Temmerman et al., 2003b). Given there is not enough evidence to differentiate whether the relationship at the study site is exponential or linear (Mogensen and Rogers, 2018), and the increase in computational demands when using a complex model structure, a decision was made to apply two simple linear relationships between modelled average inundation duration (hours per inundation event) and wetland surface elevation changes (**Figure 4**). This decision was further supported by previous ^{210}Pb analyses of lower intertidal mudflat, mangrove, and saltmarsh sediments, which showed that long-term accretion on the mudflat was higher than in saltmarsh and mangrove zones, and supported assumptions of a linear relationship (Lal, 2019).

A total of 14 visits per SET site over 20 years have been taken into account when determining the approximate surface elevation change at each SET (yellow and green symbols) shown on the y axis in **Figure 4**. These SET records have been used to construct two linear relationships that differ with respect to underlying assumptions and maximum changes in surface elevation. Linear model 1 (moderate wetland growth) presumes

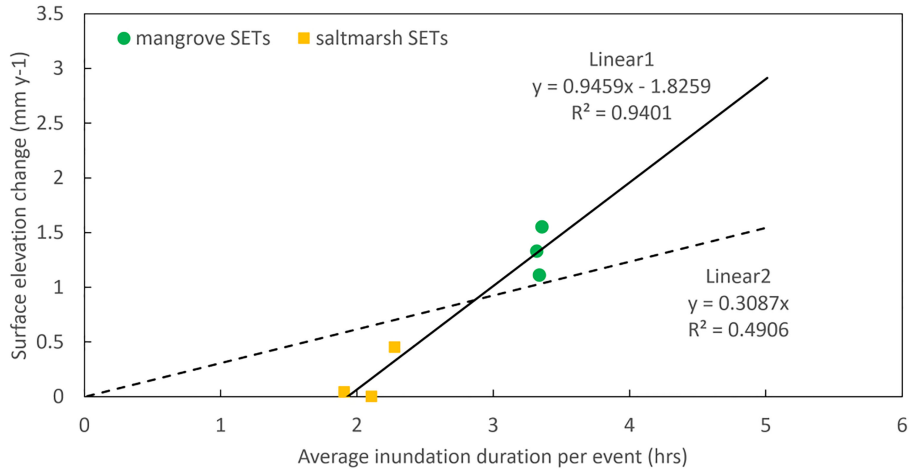

FIGURE 4 | Linear relationship between modelled average inundation duration per inundation event (hours) and wetland surface elevation change (mm yr^{-1}). Green and orange symbols are based on the six SETs with the orange squares being saltmarsh sites and the green circles representing the mangrove sites.

that sedimentation is negligible where inundation is negligible and allows for maximum elevation gains of 2.8 mm yr^{-1}, whilst linear model 2 (slow wetland growth) allows for sedimentation throughout the tidal frame and maximum increases in surface elevation of 1.5 mm yr^{-1}. Using a continuous linear relationship between inundation and sedimentation rather than separate relationships for mangrove and saltmarsh respectively, allowed for a representation of mangrove encroachment into saltmarsh as experienced at Minnamurra River and many other estuaries in southeast Australia (Chafer, 1998; Saintilan et al., 2018). The use of surface elevation change observations in WEM allows for an indirect consideration of above- and below-ground processes influencing wetland surface elevations that moderate the response of wetlands to SLR, whereas tidal simulation outputs in combination with empirical inundation tolerances adequately resembles wetland vegetation distribution. However, it is acknowledged that lower in the tidal frame where *Avicennia* and *Aegiceras* mangroves co-exist, as well as at higher elevations where saltmarsh and *Casuarina* establish, salinity may be an equally important factor for wetland species distribution (Silvestri et al., 2005). Changes in wetland distribution and surface elevation change were calculated in ArcGIS 10.7 at each coupling time step. The wetland component of the coupled modelling was verified by a combination of statistical measures (Matthew's correlation) and visual comparison of modelled wetland inundation regime at present day sea level, and the best available wetland vegetation mapping as presented in **Figure 1** (Chafer, 1998; Owers et al., 2016).

Simulated changes in intertidal wetland topography triggered by the combination of the above SLR and WEM scenarios were investigated for a selected transect approximately 1 km upstream from the entrance of the estuary (see **Figure 3**). This was undertaken by extracting surface elevations and modelled inundation regime along the same transect after topography updates at each coupling time step in ArcGIS 10.7.

3 RESULTS

3.1 Eco-Morphodynamic Model Validation

The hydrodynamic modelling setup was validated for the simulation of tidal conditions using observational field data such as water levels (**Figure 5A**), intertidal inundation depth measurements (**Figure 5B**) and flow velocities (**Table 1**). High correlation coefficients of mostly 0.99 and reasonably low RMSE in water level below 0.05 m at locations MR and further upstream confirm that the calibrated model effectively replicates tidal dynamics within the estuary (**Table 1**). However, at the entrance (G-01), modelled and observed water levels did not match as well, and this may be related to water-level fluctuations caused by ocean swell in the entrance area affecting the measurements. Modelled and observed inundation depths at locations T2Log1 – T2Log5 (**Figure 3**) correlating between 0.98 and 0.99 (RMSE's of below 0.03 m), indicate that inundation dynamics within intertidal areas are resolved adequately (**Figure 5B**). A good model performance is further shown by only small underestimations in spring tide peak flood velocities of between 0 and 0.1 m s^{-1} in upstream locations (**Table 1**).

Downstream at the entrance (G-01), peak velocity was overestimated by 1.3 m s^{-1}; however, flow velocities experienced during equipment deployment at the dynamic entrance area were considerably higher than those recorded by the bottom mounted flow meter, and thus deviations between the modelled and observed flow velocity were not surprising. The best match between modelled and observed peak velocities was achieved at location MR, which likely relates to the fact that modelling of depth averaged flow velocity is compared to observations of depth averaged rather than near-bed flow velocities due to an ADCP being used for data collection. The slight increasing trend in velocity underestimation upstream may be explained by the model domain not extending to the tidal limit of the estuary, which is due to the unavailability of

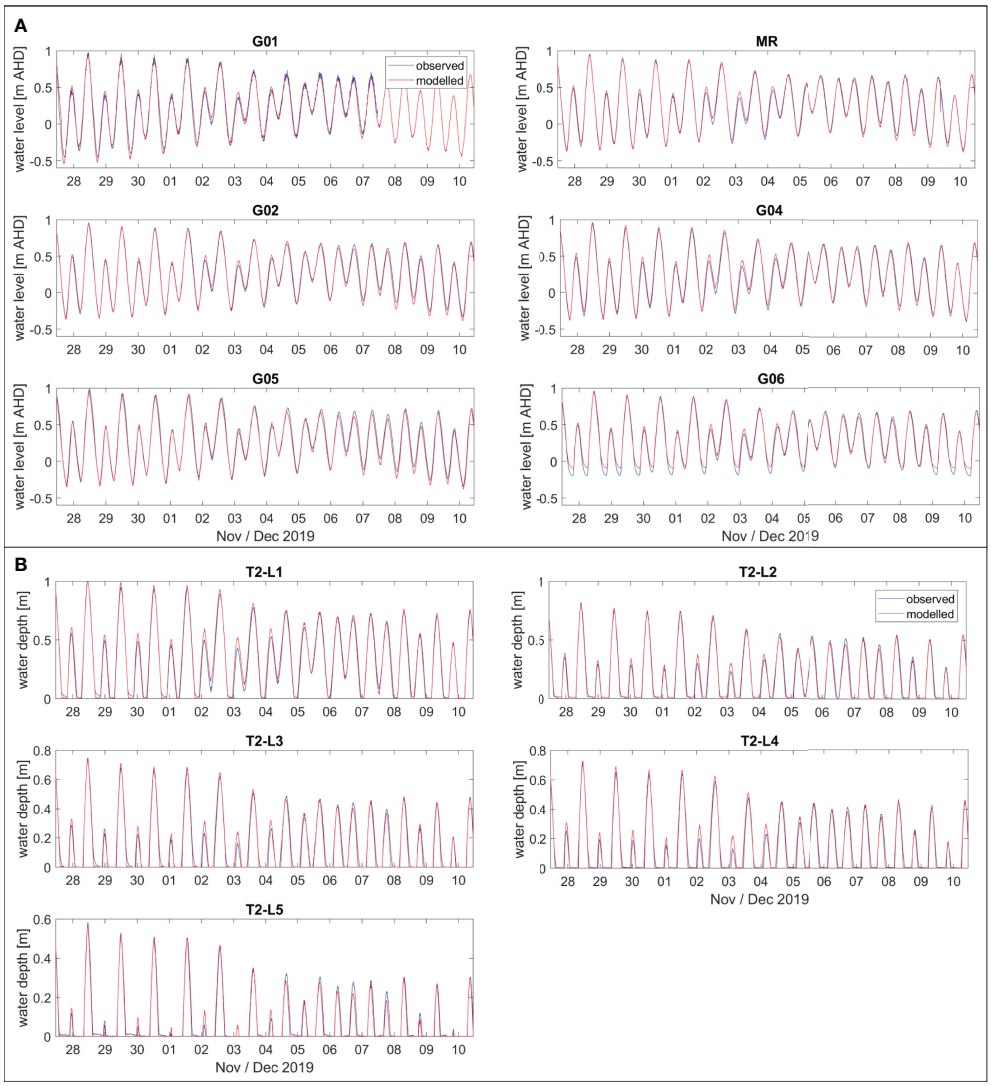

FIGURE 5 | Observed and modelled tidal water levels **(A)** and water depths **(B)** between 27 November and 10 December 2019 for monitoring locations at the Minnamurra River estuary.

TABLE 1 | Statistical measures calculated from comparison of modelled and observed flow velocities at Minnamurra River estuary. Peak velocity deviations refer to maximum over (+) and under (-) estimations by the hydrodynamic model for spring tide flood flows on 28 November 2019.

Monitoring site	r^2	RMSE (m)	Peak velocity (m s^{-1})
G-01	0.856	0.17	+1.30
MR	0.993	0.04	0.00
G-02	0.992	0.04	-0.05
G-04	0.991	0.04	-0.05
G-05	0.990	0.05	-0.10
G-06	0.988	0.05	–

This comparison was made between bottom-mounted velocity measurements and depth averaged velocity predictions except at site MR where depth-averaged ADCP measurements were obtained.

bathymetry data beyond the presented model domain. In consequence, tidal dynamics modelled upstream may have not been as variable as occurs in reality.

The predictive capability of the eco-morphodynamic model with respect to distribution patterns of mangrove and saltmarsh has been assessed by visual comparison of the best available wetland mapping (**Figure 6A**) with model predictions of mangrove and saltmarsh distribution based on simulated hydrodynamics (28 days) at contemporary sea level (**Figure 6B**).

Model predictions of mangrove distribution visually correlate well with the observed distribution patterns for floodplains surrounding Rocklow Creek in the north, the central floodplain and most of the southern floodplain. Small deviations in mangrove

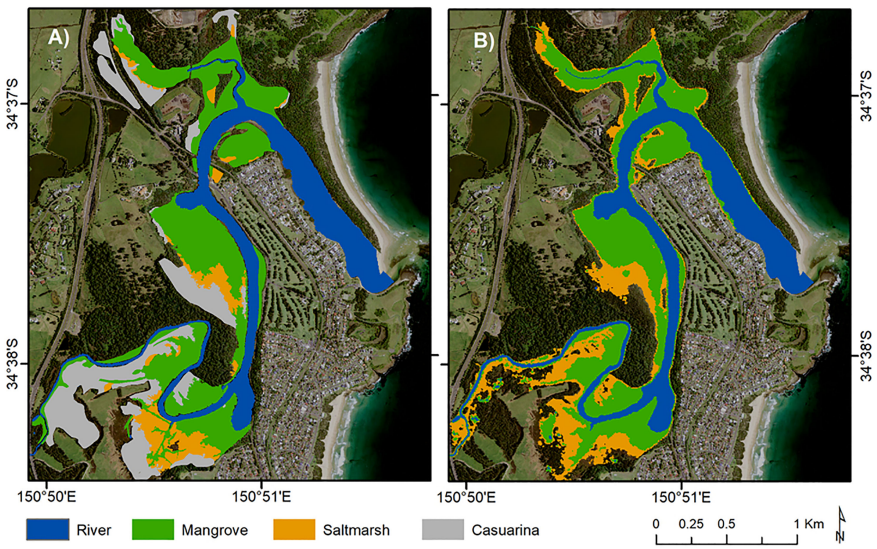

FIGURE 6 | Comparison of wetland vegetation mapping based on Owers et al. (2016) **(A)** and eco-morphodynamic model predictions of mangrove and saltmarsh distribution **(B)** based on average inundation durations per event from a 28-day tide simulation for November/December 2019. Note that *Casuarina* are not included in the model.

distribution were observed at the southern floodplain where tidal creeks with a width of less than 5 m and mostly unknown bathymetry intersect the floodplain, which were not properly resolved by the mesh grid and resulted in an over-representation of mangroves in these areas. Model predictions of saltmarsh distribution with the wetland mapping correlate well at the boundary to the mangrove zone, but saltmarsh distribution appears more extensive in the landward direction where the wetland mapping mostly suggests *Casuarina* forest. A field survey in these areas revealed that most of the *Casuarinas* that are predicted to be saltmarsh by the model, have saltmarsh beneath the *Casuarina* canopy (also reported by Oliver et al., 2012), and consequently the model predictions can be interpreted as reasonable. RTK-GPS measurements showed that these sites share surface elevations similar to those occupied by saltmarsh in nearby locations. Above outlined issues regarding the mapping of saltmarsh also impacted the calculation of Matthew's correlation coefficient (0.52); however, predictions of contemporary mangrove and saltmarsh areas were overall good (accuracy of 84%).

3.2 Eco-Morphodynamic Modelling Results

3.2.1 Intertidal Wetland Topography Response to SLR

Vertical changes in intertidal wetland topography were greatest for low SLR simulations coupled with WEM Linear 1, and at elevations low in the tidal frame (**Figure 7A**). To assist with interpretation of changes in wetland topography, **Figure 7** also includes simulated average inundation durations (per event) and corresponding wetland vegetation configurations under SLR.

At a distance along the transect of 100 m, large increases in surface elevation of up to 0.18 m by 2100 were modelled for the lower SLR simulation (RCP2.6) and WEM Linear 1, which is presently at an elevation below 0.2 m AHD (**Figure 7A**). By contrast, predictions of surface elevation from the higher SLR scenario (RCP8.5) for the same location were 0.08 m, suggesting slower vertical changes under the higher SLR scenario. Higher in the tidal frame (above 0.4 m AHD present elevation), gains in wetland surface elevation were quite similar for both SLR scenarios (approximately 0.1 m); however, from an elevation of 0.5 m AHD (present day), surface elevation increased at a higher rate considering the higher SLR scenario.

Predictions of topographic change for SLR simulations coupled with WEM Linear 2 showed similar spatial patterns with respect to differences between the lower and higher SLR scenario (**Figure 7B**). Overall vertical changes were approximately half of those described above, except for slightly greater elevation gains (up to 0.04 m) high in the tidal frame (above 0.5 m AHD present level) for simulations of the low SLR scenario. Analyses of changes in intertidal wetland topography from another profile located in the vicinity of tide gauge G-03 (see **Figure 3** for location) reinforces above described trends in adjustments of intertidal wetland topography in response to SLR (**Supplementary Figure 5**).

3.2.2 Tidal Range Response to SLR

Tidal dynamics in the main channel of the estuary were affected by SLR and differed spatially (lower and upper estuary), but also between simulations of the low and high SLR scenarios (**Figure 8**). For the simulation of low SLR and WEM Linear 1, tidal range increased linearly with SLR by approximately 0.01 m every 10 years, with total increases of + 0.08 m at the downstream location MR and + 0.09 m at the upstream location G04. For the high SLR simulation, tidal range was shown to

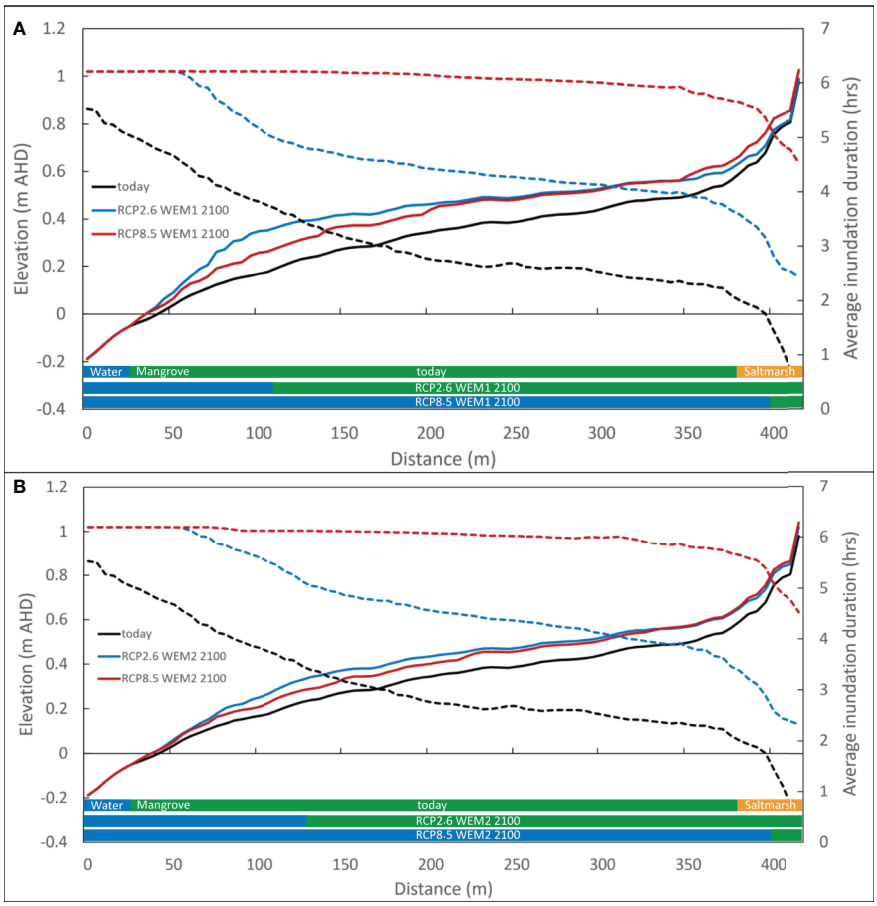

FIGURE 7 | Topographic changes in response to SLR for a selected intertidal wetland transect (see **Figure 3** for location) as of today (black), for the simulation of the low SLR (blue) and high SLR (red), as well as WEM Linear 1 (panel **A**) and Linear 2 (panel **B**). Blue, green and orange bars at the bottom of each panel indicate wetland vegetation configurations resulting from changing wetland inundation regimes under the different scenarios. Dashed lines represent the simulated average inundation duration (per event) corresponding to each scenario.

initially increase linearly (+ 0.11 m and + 0.09 m up- and downstream by 2080, respectively), but remain unchanged or decrease after sea level exceeded an increase of 0.6 m. Absolute increases in tidal range by 2100 are projected to translate into relative increases of approximately 6-7% for the lower SLR scenario and 7-8% for the higher SLR scenario compared to 2020 levels. Projections of tidal range under SLR coupled with WEM Linear 2 were almost identical (+/- 1-2 mm) to the patterns described above (**Figure 8B**).

3.2.3 Mangrove and Saltmarsh Response to SLR

The choice of SLR and wetland elevation adjustment scenario influenced the model outputs. The differences in distributional patterns of mangrove and saltmarsh for each scenario are described below (**Figure 9**). For WEM Linear 1 under a low SLR scenario (RCP2.6) mangroves adjusted to rising sea level for most of the century and expanded landward into saltmarsh when mean sea level exceeded an increase of 0.2 m (which corresponds to a surface elevation of 0.3 m AHD) (**Figure 9**). After this, mangrove at elevations <0.2 m AHD converted to open water due to the increasing inundation, which was particularly observed where the intertidal topography is gently sloped (e.g. shallow bays at the north of the central floodplain (**Figure 10**) and east of the southern floodplain). Saltmarsh expanded landward for WEM Linear 1 under simulation of low SLR; however, net changes in total saltmarsh extent were minimal due to the expansion of mangroves into lower elevation saltmarsh.

Changes in the ratio of mangrove, saltmarsh and open water (**Figure 11** – solid lines) indicate that overall the extent of mangroves and open water increased gradually over the century (+ 43% and + 31% respectively), whereas saltmarsh extent increased marginally (+ 6%). However, the model did not include the full intertidal extent under the highest SLR scenarios at 2100 due to an absence of suitable bathymetry data in the most upstream areas which are currently not tidally influenced.

For WEM Linear 1 under high SLR (RCP8.5) mangroves expanded in a landward direction into saltmarsh throughout the simulation period, which resulted in an overall increase of 70% in mangrove coverage. Most of this increase in mangrove area

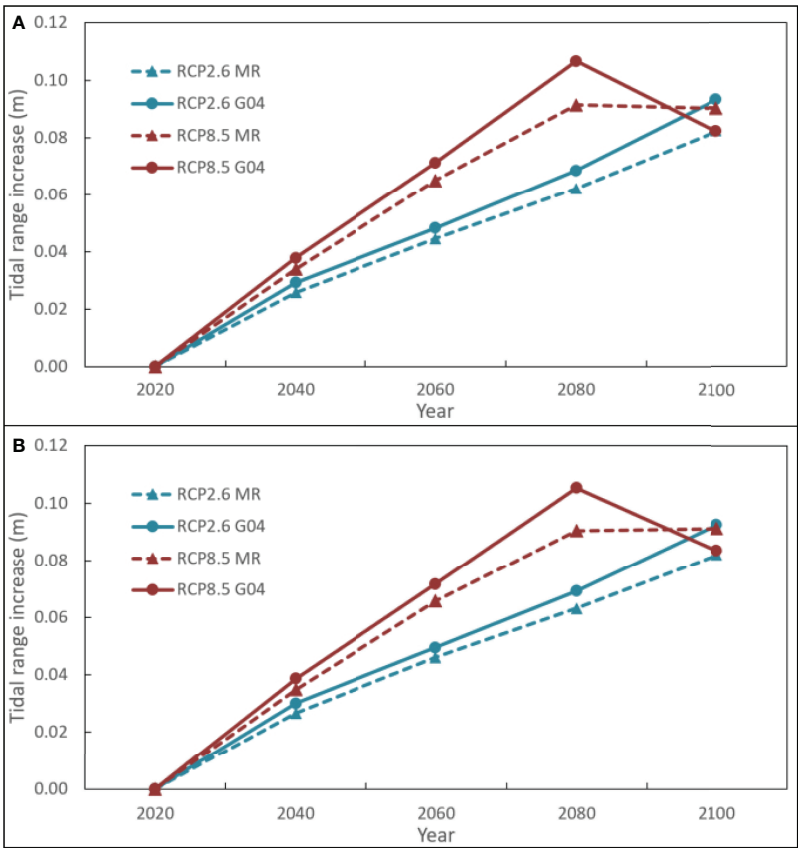

FIGURE 8 | Increases in spring tidal range under low (blue) and high SLR (red) for an upstream (G04 –solid lines) and downstream location (MR – dashed lines), as well as WEM Linear 1 (panel **A**) and Linear 2 (panel **B**). See **Figure 3** for the exact location of both monitoring sites. Values are with respect to maximum spring tidal range modelled for 2020.

occurred in the upper estuary surrounding the southern floodplain and further upstream (**Figure 9**). Mangroves further downstream appeared to be subject to coastal squeeze and were not projected to expand to higher elevations because the topography of the central and northern floodplain inhibited their establishment (**Figure 10**).

Under high SLR and WEM Linear 1, saltmarsh expanded landward but its total extent increased marginally (+ 4%). A large increase in open water extent was observed once mean sea level exceeded 0.5 m (corresponding to a surface elevation of 0.6 m AHD), which totalled to an increase in these areas of + 169% by 2100. This large increase in open water areas resulted in a shift in the proportion of mangrove, saltmarsh and open water areas, with a domination of open water areas from approximately 2070 under high SLR (**Figure 11A** – dashed lines).

Projections of wetland distribution for SLR simulations and WEM Linear 2 were very similar to those of WEM Linear 1 (**Figure 9** and **Figure 11B**). Under a low SLR scenario, open water areas were marginally larger by the end of the century (+ 5.6%), mangrove areas slightly smaller (- 3.6%), whereas saltmarsh extents were slightly larger mid-century (+ 4.3-7.3%) and largely unchanged by 2100 (- 0.2%). Similar trends were observed using a high SLR scenario and WEM Linear 2, except for slightly larger saltmarsh extents by 2100 (+ 4.7%).

4 DISCUSSION

4.1 Wetland and Tidal Regime Responses to SLR at Minnamurra

This analysis demonstrated that the rate of SLR affects wetland elevation adjustment, wetland inundation regimes, and the lateral distribution of wetland vegetation. At the same time, changes in wetland distribution also alter tidal hydrodynamics. These projections were only achieved by coupling tidal hydrodynamics to a model of wetland elevation adjustment developed for this study (i.e. WEM). High correlation coefficients and low RMSEs between observed and modelled water levels and wetland inundation, and reasonable correlation and accuracy between detailed wetland mapping and model projections of mangrove and saltmarsh at contemporary sea level, provided considerable confidence that the model setup was appropriate.

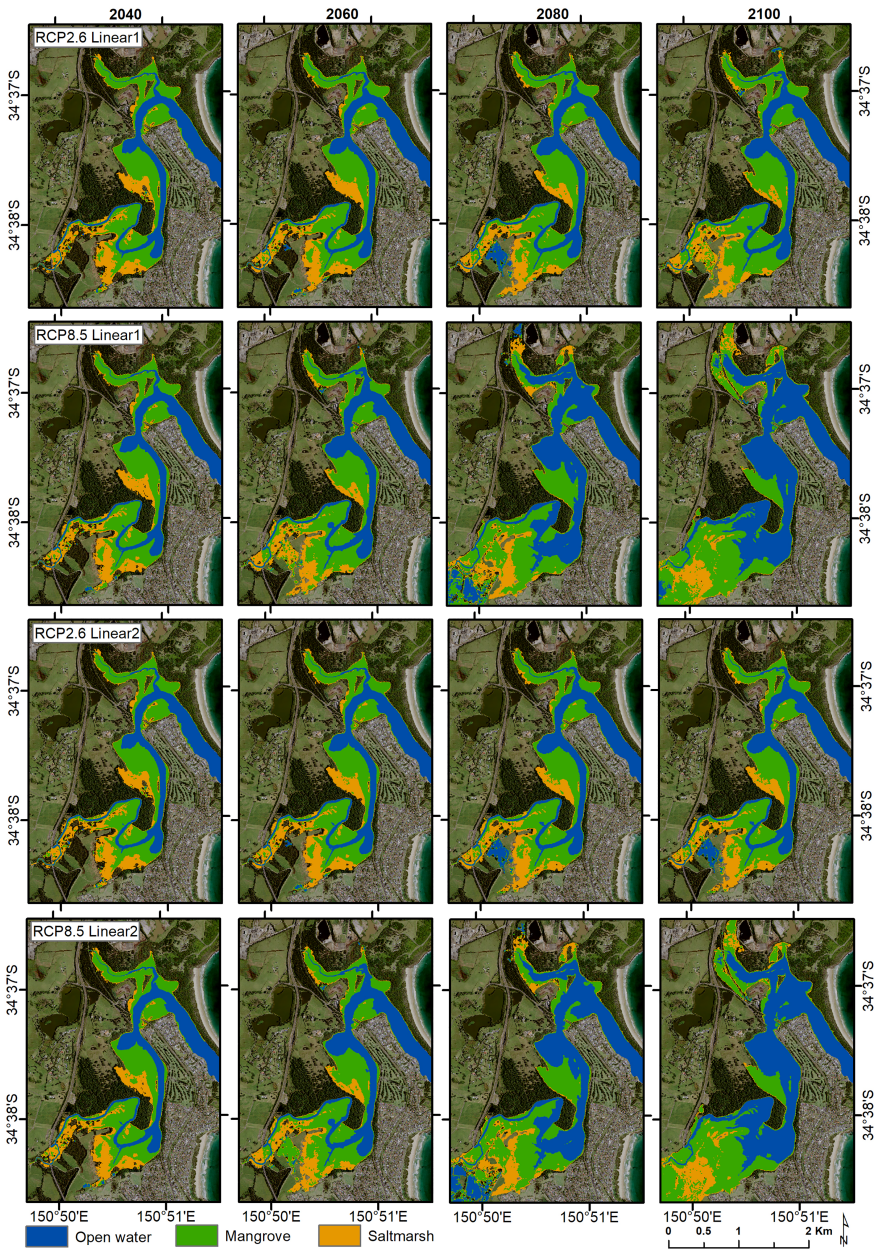

FIGURE 9 | Projections of intertidal wetland vegetation communities (mangrove and saltmarsh) for low and high SLR scenarios, as well as WEM scenarios Linear 1 and Linear 2.

Modelling of four simulations including low (RCP2.6) and high (RCP8.5) SLR scenarios, as well as two wetland adjustment scenarios (Linear 1 and Linear 2), showed consistent patterns of mangroves expanding into saltmarsh, saltmarsh transitioning to higher elevations (currently occupied by *Casuarina* forest), and substantially larger open water areas at relatively high rates of SLR.

Simulations using the lower SLR scenario indicate that tidal wetlands adjust to rising sea levels by increasing substrate elevation (up to 0.18 m) and by vegetation transitions to higher elevations, leading to an increase in extent, particularly for mangroves (+ 43%). Only mangroves positioned lower in the tidal frame converted to open water areas, whereas higher in the tidal frame mangroves replaced saltmarsh due to increasing tidal inundation. This modelled encroachment of mangroves into saltmarsh has been observed in the field in recent decades and attributed to SLR (Chafer, 1998; Saintilan and Rogers, 2013; Saintilan et al., 2018). The ability of mangroves to withstand comparatively lower rates of SLR, as shown here (modelling of SLR + 5mm yr^{-1}), aligns well with previous suggestions that

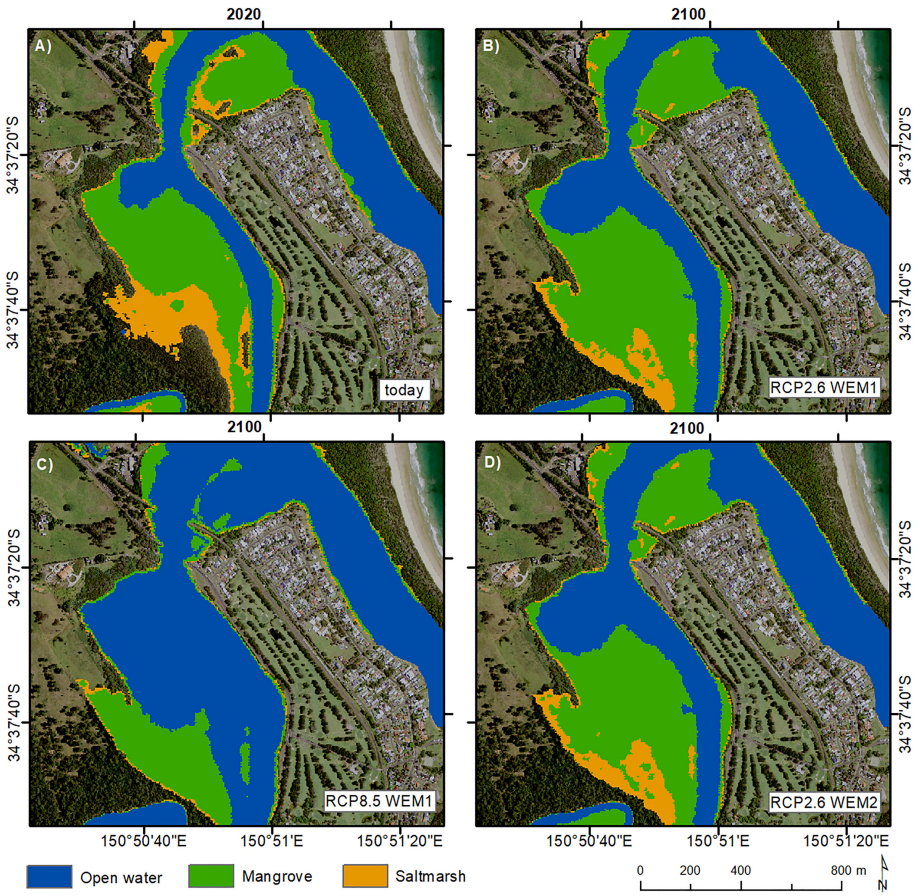

FIGURE 10 | Projections of intertidal wetland vegetation communities (mangrove and saltmarsh) for today **(A)**, WEM1 and low SLR **(B)**, WEM1 and high SLR **(C)**, and WEM2 and low SLR **(D)**.

mangroves may tolerate increases in the rate of mean sea level rise of up to 7 mm yr^{-1} (Saintilan et al., 2020). Saltmarsh expanded to higher elevations where tidal inundation was sufficient (+ 6% in coverage by 2100), which appears to be only on the southern floodplain. Saltmarsh, being preferentially located in the upper intertidal, was more sensitive to coastal squeeze than mangroves.

Simulations using the higher SLR scenario indicated that the ability of mangroves to adjust to SLR decreases when the rate of sea-level rise accelerates (> 10 mm yr^{-1} and up to 14 mm yr^{-1} at the end of the century), which was particularly shown during the last quarter of the century when low elevated mangroves mainly converted to open water areas (**Figures 9**, **10** and **11**). Nevertheless, mangrove areas overall substantially expanded (+ 70%), whereas landward expansion of saltmarsh resulted in only a minor increase in coverage (+ 4%). Differences in wetland resilience between low and high SLR simulations presented here show parallels to SLAMM modelling for lagoon marshes in Portugal by Carracso et al. (2021) who demonstrated a non-linearity in wetland response to SLR and critical thresholds when wetland systems are no longer in pace with SLR.

The selection of wetland adjustment scenarios (Linear 1 and Linear 2) marginally affected projections of mangrove, saltmarsh and open water area extents under SLR (+/- 5%); however, comparison between scenarios showed how assumptions regarding sedimentation influence model outcomes, with WEM Linear 1 simulations (moderate wetland growth) showing greater mangrove resilience and less open water conversion. Simulations of WEM Linear 2 (slow wetland growth) projected mangroves to be more vulnerable to SLR and saltmarsh to be more resilient to SLR. These differences relate to differences in WEM Linear 1 and WEM Linear 2 for low inundation durations. WEM Linear 1 did not allow for sedimentation for low inundation durations characteristic of much of the saltmarsh extent (**Figure 4**).

Wetland dynamics under SLR as projected by the eco-morphodynamic model show some parallels but also differences with earlier modelling for selected sites at Minnamurra River estuary (Oliver et al., 2012; Mogensen and Rogers, 2018). For example, spatial modelling by Oliver et al. (2012) has indicated that mangrove and saltmarsh on the central floodplain may be able to withstand a lower rate of SLR, but conversion of low elevation mangroves to open water areas and

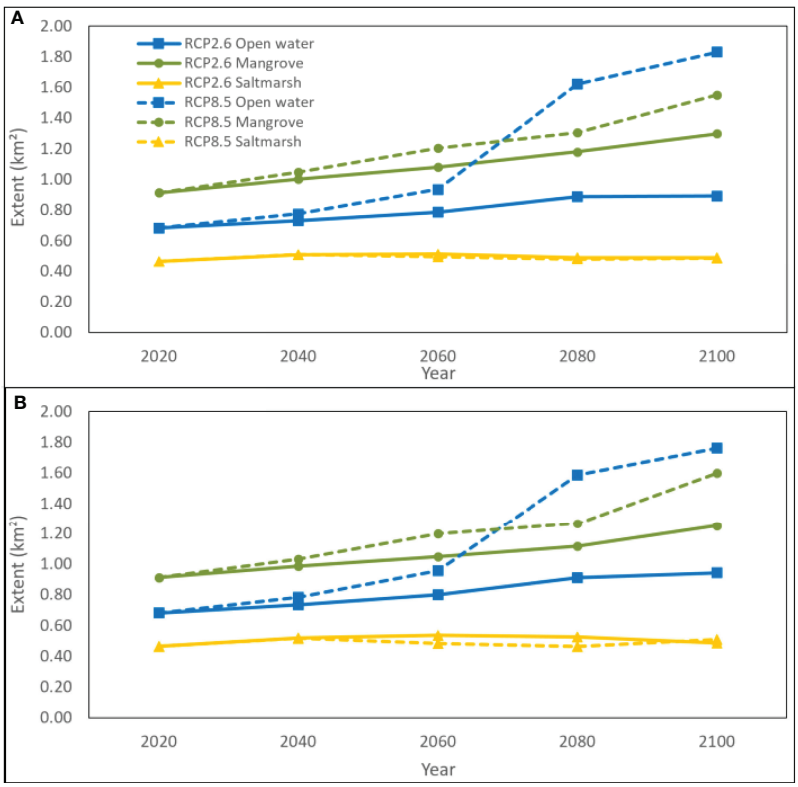

FIGURE 11 | Projections of river (blue squares), mangrove (green circles) and saltmarsh (orange triangles) extents in response to the lower RCP2.6 SLR scenario (solid) and the higher RCP8.5 SLR scenario (dashed) for WEM scenarios Linear 1 (panel **A**) and Linear 2 (panel **B**).

replacement of lower elevation saltmarsh by mangroves expanding landward under a higher rate of SLR. Similar wetland responses to high rates of SLR for the central floodplain were indicated by Mogensen and Rogers (2018) using SLAMM and two empirically-based spatial models following methods presented by Oliver et al. (2012) and Temmerman et al. (2003b). However, exponential modelling by Mogensen and Rogers's (2018) that projects mangroves largely adjusting to SLR on the southern floodplain differs substantially from results here, indicating a conversion of low elevation mangroves to open water areas. A potential explanation for this stronger mangrove resilience suggested by Mogensen and Rogers (2018) could be the exponential relationship for vertical accretion underlying one of their empirical spatial models (after Temmerman et al., 2003), which facilitates much higher sedimentation and surface elevation gains than the linear relationship between wetland inundation regime and surface elevation change applied here. There is increasing evidence that organic matter additions at lower elevation occupied by mangroves may provide substantial sedimentation contributions justifying an exponential model structure (Morris et al., 2002; Kirwan and Murray, 2007; Rogers and Saintilan, 2021), however given the lack of field data supporting such relationships at Minnamurra, the Linear WEMs presented here appear to be the best approximations. We acknowledge that this linear model structure influences the model outcomes and conclusions of this study, and that using an exponential model structure would likely increase the resilience of mangroves low in the tidal frame; however, previous ^{210}Pb analysis of low elevated mangroves has not suggested high accretion rates supporting the use of an exponential model structure (Lal, 2019).

Projections of intertidal wetland topography illustrate how the rate of SLR and assumptions regarding wetland elevation change (WEM Linear 1 and Linear 2) influence wetland geomorphology in response to SLR (**Figure 7** and **Supplementary Figure 5**). When the rate of SLR is low and wetland elevation change was assumed to be moderate (Linear 1), mangroves positioned low in the tidal frame adjusted to rising sea level by increasing in surface elevation (by up to 0.18 m), and in consequence the intertidal geomorphology became increasingly horizontal and developed towards a platform with a flat profile. This can be explained by mangroves lower in the tidal frame increasing surface elevation throughout the simulation period under the low SLR scenario (80 years), whereas under high SLR scenario, positions in the tidal frame suitable for mangroves shifted upwards and thus gains in surface elevation eventually stopped when mangroves converted to open water areas. It is acknowledged that treating tidal flats as static substrates does not represent reality as sediment supply may allow tidal flats to increase elevation at a rate similar to SLR; however, the WEM was not parameterised to model main-channel

morphodynamics or tidal flat vertical adjustments. Model simulations assuming low rates of wetland elevation adjustment (Linear 2) projected approximately 50% smaller gains in wetland surface elevation, but slightly higher saltmarsh resilience under low SLR due to the construction of the linear relationship.

Simulations for both SLR scenarios indicated that hydrodynamics of the estuary change in response to rising sea level, with tidal range shown to increase by up to 8% (**Figure 8**). Under both SLR scenarios, tidal range appeared to increase linearly with SLR; however, simulations using the higher SLR scenario indicated downstream stabilisation and upstream decline in tidal range when SLR exceeded 0.6 m, which coincides with the conversion of large mangrove areas low in the tidal frame to open water areas (**Figure 11**). This non-linear behaviour of tidal range under high SLR may be explained by substantial widening of the main channel along with increased intertidal storage areas, which have been associated with tidal energy dissipation and potential reduction in tidal range under SLR (Du et al., 2018; Kumbier et al., 2018a). This is an important finding given the significant role of tidal range as a parameter of wetland functioning and since many wetland modelling studies assume a constant tidal range when estimating wetland response to SLR. Even though absolute changes in tidal range were comparatively small (+ 0.1 m), due to the micro-tidal regime of Minnamurra River, such alterations in tidal range can increase the vertical space available for wetland establishment, lengthen the duration of inundation, and thus impact modelling outcomes. Therefore, it is proposed that wetland modelling in estuaries similar to the one presented here should account for alteration in tidal regime, which may be particularly important for meso- and macro-tidal systems as absolute changes in tidal range will likely be of greater magnitude than results presented here and justify the extra complexity added by considering wetland sedimentation.

4.2 Modelling Implications

In this study, such consideration of alteration in tidal dynamics was achieved by coupling a depth averaged hydrodynamic model with an empirical wetland elevation model. This approach allowed for inclusion of interrelations between hydrodynamics, wetland extent and intertidal geomorphology, which have been shown to be responsible for alteration and non-linear responses in tidal range observed here. Integrating modelling approaches can account for these eco-geomorphological feedbacks between estuarine hydrodynamics and intertidal wetlands, which should be considered when modelling wetland response to SLR at the scale of an estuary. This is particularly important for infilled channelised estuaries, like Minnamurra River, where main channel hydrodynamics and intertidal wetlands have been shown to be interconnected (Kumbier et al., 2022). In these estuaries, tides may be amplified before dissipating along the estuary, which occurs as an outcome of main channel hydrodynamics and propagation of tides across intertidal wetlands.

The eco-morphodynamic model presented here differs from previous coupled hydrodynamic-wetland models in the way it accounts for tidal modifications. Whereas previous studies utilised hydrodynamic modelling to produce generalised tidal water levels (e.g. MHW) to delineate wetland zonation (Alizad et al., 2016a; Rodríguez et al., 2017), the framework presented in this study calculates spatially explicit estimates of wetland inundation regime that are explicitly linked to vegetation occurrence. This procedure is an advancement given the spatial variability of tides along an estuary, and the influence of vegetation on tidal flow in wetlands (Mazda et al., 1995; Temmerman et al., 2005). However, it is acknowledged that the representation of bottom roughness could be improved by incorporation of depth-dependent coefficients considering the effects of vegetation structure (Mazda et al., 1997), such as used in more detailed small scale studies (Horstmann et al., 2015; Horstmann et al., 2021). This simplification of bottom roughness in the present study could have affected projections of tidal dynamics in response to SLR, also because a replacement of mangrove areas with open water would most likely imply a transitional time where woody mangrove biomass slowly decomposes and continues to interact with tidal flow. Consideration of site-specific changes in wetland surface elevation from 20 years of observation utilising SETs provides a robust foundation to extrapolate trends in surface elevation change using hydrodynamic modelling. The comparatively simple wetland adjustment model used here (i.e. WEM) allows for indirect consideration of mineral and organic matter accumulation, as well as below-ground processes, such as auto-compaction. Whereas the presented model structure assumes that sedimentation on estuarine wetlands is fully independent of temporal and spatial sediment availability, more realistic future projections could be achieved by considering changes in sediment transport and availability in response to SLR to account for processes, such as sediment dispersion resuspension, within the estuary and wetlands (e.g. using a 3D hydrodynamic-sediment transport model); however, such considerations add considerable complexity and computational demands due to the 3D model structure.

Trade-offs between model complexity and over-parameterisation are a known challenge of coupled hydrodynamic-ecological estuarine models (Ganju et al., 2016), and model design should be driven by the purpose of the modelling framework. This study aimed to develop a reduced complexity wetland model framework with improved representation of estuarine hydrodynamics, which is transferable to other locations provided sufficient data is available to empirically define a wetland elevation model. This transferability is achieved by determining wetland response to SLR based on modelling of inundation regimes, which allows for consideration of any wetland vegetation as long as inundation preferences are known. The procedures of the eco-morphodynamic model presented in this study can be adopted for wetland vulnerability assessments in other estuarine environments providing reliable wetland surface elevation trajectories are available (e.g. from SETs or sediment dating); however, model results for estuarine wetlands where vertical accretion is dominated by tidal supply of mineral sediments may be limited, as the model does not specifically account for mineral sediment transport within the estuary and wetlands.

In this study supratidal wetlands of *Casuarina* forest were not considered despite evidence of saltmarsh beneath forest canopies, modelled evidence of saltmarsh encroachment upon supratidal forests elsewhere, and that *Casuarina* may have capacity to adjust to rising sea level (Rogers et al., 2019b). However, too little is

known about their response to SLR to adequately parameterise the WEM, and further research of the vertical adjustment of these forests is required to understand their behaviour under SLR and to consider them in future modelling studies of wetland response to SLR. Additionally, the interconnections between estuarine hydrodynamics and intertidal wetlands demonstrated here, suggest that studies into tidal hydrodynamics in estuaries (e.g. flow velocities, asymmetry) can be affected by intertidal geomorphology. Whilst it has been known and researched for some time (Aubrey and Speer, 1985; Friedrichs and Aubrey, 1988; Friedrichs et al., 1990), widespread adoption of modelling approaches that recognise the interconnection between tidal hydrodynamics and geomorphology has not occurred. Modelling results here align with similar modelling of estuarine marshes in the US (Donatelli et al., 2018), and show how intertidal geomorphology may change in response to SLR, which demonstrably affected tidal range. It is anticipated that the response of entrance morphology and sub-tidal channel morphology to SLR, not simulated here, will also cause morphodynamic feedbacks that affect tidal range. Similarly, other tidal properties, such as velocity or asymmetry, may be affected by changing intertidal wetland geomorphology under SLR; however, these effects are yet to be sufficiently quantified and previous SLR modelling studies have predominantly focussed on hydrodynamics only. Effective planning and decision making for SLR in estuaries would benefit from simultaneous investigation of estuarine and intertidal wetland processes.

5 CONCLUSIONS

Eco-morphodynamic modelling at Minnamurra River estuary has demonstrated that the fate of intertidal wetlands depends on the rate of SLR, with projections based on slow SLR (+ 5mm yr^{-1}) indicating mangroves may adjust to SLR, but when exposed to a higher rate of SLR (> 10mm yr^{-1}) conversion of low elevated mangroves to open water areas were projected. Within model scenarios, tidal range inside the estuary was shown to increase overall under low and high SLR (by up to + 8%), and to respond non-linearly to high SLR. This non-linear response may be related to eco-geomorphological feedbacks caused by changing wetland extents and intertidal geomorphology. As low elevated mangrove areas convert to open water, tidal energy dissipates in intertidal storage areas and reduces tidal range. Model projections of mangrove and saltmarsh distribution and their associated rates of wetland elevation adjustment are a function of SLR, with feedbacks demonstrated between the ecology, morphology and hydrodynamics. Comparisons of model simulations based on two SLR scenarios and two wetland elevation adjustment scenarios indicate that macrophyte distribution at Minnamurra River is highly dependent upon the rate of SLR and its influence on wetland elevation adjustment.

Whereas many wetland modelling studies of responses to SLR assume tidal range to remain unchanged, modelling in this study indicates that hydrodynamics in estuaries, such as tidal range, can alter in response to SLR, if entrance and channel morphology do not change elevation significantly in response to SLR. Integrated modelling approaches, such as the coupled eco-morphodynamic model presented here, are required to account for the dynamic eco-geomorphological feedbacks resulting from the interaction of estuarine hydrodynamics and intertidal wetlands under SLR. More generally, incorporating hydrodynamic modelling into wetland research as applied here allows for a spatially explicit calculation of wetland inundation regimes, which improves the representation of tidal inundation in wetland modelling. Altogether these improvements in intertidal flow representation and consideration of tidal responses to SLR advance modelling of wetland response to SLR in estuaries, and may contribute to better understanding and management of estuarine-wetland systems.

DATA AVAILABILITY STATEMENT

The modelling output data supporting the conclusions of this article will be made available by the authors upon request.

AUTHOR CONTRIBUTIONS

KK, KR, MH and CW conceived and designed the study. KK, MH, KL, LM and KR collected and analysed the field data. KK set-up the modelling and ran the simulations. KK, KR, MH and CW analysed and interpreted the modelling results. KK wrote the paper with substantial input from KR, MH and CW. All authors contributed to the article and approved the submitted version.

FUNDING

The University of Wollongong and the NSW Department of Planning, Industry and Environment provided financial support for this research.

ACKNOWLEDGMENTS

KK expresses gratitude to the University of Wollongong and the NSW Department of Planning, Industry and Environment for supporting his PhD research with a scholarship. The authors thank everyone who contributed to the SET data collection and analysis in the past 20 years, and the School of Aviation at the University of New South Wales for the provision of LiDAR data. The authors acknowledge the Dharawal people who are the traditional custodians of the Minnamurra River catchment area.

SUPPLEMENTARY MATERIAL

The Supplementary Material for this article can be found online at: https://www.frontiersin.org/articles/10.3389/fmars.2022.860910/full#supplementary-material

REFERENCES

Alizad, K., Hagen, S. C., Medeiros, S. C., Bilskie, M. V., Morris, J. T., Balthis, L., et al. (2018). Dynamic Responses and Implications to Coastal Wetlands and the Surrounding Regions Under Sea Level Rise. *PloS One* 13, 1–27. doi: 10.1371/journal.pone.0205176

Alizad, K., Hagen, S. C., Morris, J. T., Bacopoulos, P., Bilskie, M. V., Weishampel, J. F., et al. (2016a). A Coupled, Two-Dimensional Hydrodynamic-Marsh Model With Biological Feedback. *Ecol. Modell.* 327, 29–43. doi: 10.1016/J.ECOLMODEL.2016.01.013

Alizad, K., Hagen, S. C., Morris, J. T., Medeiros, S. C., Bilskie, M. V., and Weishampel, J. F. (2016b). Coastal Wetland Response to Sea-Level Rise in a Fluvial Estuarine System. *Earth's Futur.* 4, 483–497. doi: 10.1002/2016EF000385

Alizad, K., Medeiros, S. C., Foster-Martinez, M. R., and Hagen, S. C. (2020). Model Sensitivity to Topographic Uncertainty in Meso- And Microtidal Marshes. *IEEE J. Sel. Top. Appl. Earth Obs. Remote Sens.* 13, 807–814. doi: 10.1109/JSTARS.2020.2973490

Allen, J. R. L. (2000). Morphodynamics of Holocene Salt Marshes: A Review Sketch From the Atlantic and Southern North Sea Coasts of Europe. *Quat. Sci. Rev.* 19, 1155–1231. doi: 10.1016/S0277-3791(99)00034-7

Arcement, G. J., and Schneider, V. R. (1989). *Guide for Selecting Manning's Roughness Coefficients for Natural Channels and Flood Plains, US Geological Survey Water-Supply Paper 2339*. Available at: https://doi.org/10.3133/wsp2339.

Aubrey, D. G., and Speer, P. E. (1985). A Study of non-Linear Tidal Propagation in Shallow Inlet/Estuarine Systems Part I: Observations. *Estuar. Coast. Shelf Sci.* 21, 185–205. doi: 10.1016/0272-7714(85)90096-4

Baltzer, F. (1969). Les Formations Végétales Associés Au Delta De La Dumbea (Nouvelles Calédonies) Et Leurs Indications Écologiques, Géomorphologiques Et Sédimentologiques Mises En Évidence Par La Cartographie. *Ser. Géol.* 1, 59–84.

Barbier, E. B., Sally, D. H., Chris, K., Evamaria, W. K., Adrian, C. S., and Brian, R. S. (2011). The Value of Estuarine and Coastal Ecosystem Services. *Ecol. Monogr.* 81, 169–193. doi: 10.1890/10-1510.1

Benson, T. (2020). *Telemac Tools* (MATLAB Central File Exchange). Available at: https://www.mathworks.com/matlabcentral/fileexchange/25021-telemac-tools (Accessed 12.16.20).

Cahoon, D. R., Hensel, P. F., Spencer, T., Reed, D. J., McKee, K. L., and Saintilan, N. (2006). "Coastal Wetland Vulnerability to Relative Sea-Level Rise: Wetland Elevation Trends and Process Controls," in *Wetlands and Natural Resource Management*. Eds. J. T. A. Verhoeven, B. Beltmn, R. Bobbink and D. F. Whigham (Berlin, Germany: Springer Heidelberg), 271–292. doi: 10.1007/978-3-540-33187-2_12

Cahoon, D. R., Lynch, J. C., Hensel, P., Boumans, R., Perez, B. C., Segura, B., et al. (2002). High-Precision Measurements of Wetland Sediment Elevation: I. Recent Improvements to the Sedimentation-Erosion Table. *J. Sediment. Res.* 72, 730–733. doi: 10.1306/020702720730

Cahoon, D. R., Perez, B. C., Segura, B. D., and Lynch, J. C. (2011). Elevation Trends and Shrink-Swell Response of Wetland Soils to Flooding and Drying. *Estuar. Coast. Shelf Sci.* 91, 463–474. doi: 10.1016/j.ecss.2010.03.022

Cahoon, D. R., and Reed, D. J. (1995). Relationships Among Marsh Surface Topography, Hydroperiod, and Soil Accretion in a Deteriorating Louisiana Salt Marsh. *J. Coast. Res.* 11, 357–369. doi: 10.2307/4298345

Carrasco, A. R., Kombiadou, K., Amado, M., and Matias, A. (2021). Past and Future Marsh Adaptation: Lessons Learned From the Ria Formosa Lagoon. *Sci. Total Environ.* 790, 148082. doi: 10.1016/j.scitotenv.2021.148082

Chafer, C. J. (1998). A Spatio-Temporal Analysis of Estuarine Vegetation Change in the Minnamurra River 1938 - 1997. *Rep. Minnamurra Estuary Manage. Committee.* 47pp.

Chow, V. T. (1959). *Open-Channel Hydraulics, Science*. (Europe, New York, USA: McGraw-Hill Education).

Church, J. A., Clark, P. U., Cazenave, A., Gregory, J. M., Jevrejeva, S., Levermann, A., et al. (2013). Chapter 13: Sea Level Change, IPCC. *Am. Assoc. Adv Sci.* 1535pp. doi: 10.1126/science.342.6165.1445-a

Craft, C., Clough, J., Ehman, J., Joye, S., Park, R., Pennings, S., et al. (2009). Forecasting the Effects of Accelerated Sea-Level Rise on Tidal Marsh Ecosystem Services. *Front. Ecol. Environ.* 7, 73–78. doi: 10.1890/070219

D'Alpaos, A., Lanzoni, S., Marani, M., and Rinaldo, A. (2007). Landscape Evolution in Tidal Embayments: Modeling the Interplay of Erosion, Sedimentation, and Vegetation Dynamics. *J. Geophys. Res.* 112, F01008. doi: 10.1029/2006JF000537

Dangendorf, S., Marcos, M., Wöppelmann, G., Conrad, C. P., Frederikse, T., and Riva, R. (2017). Reassessment of 20th Century Global Mean Sea Level Rise. *Proc. Natl. Acad. Sci. U. S. A.* 114, 1–6. doi: 10.1073/pnas.1616007114

Department of Planning Industry and Environment (2017). *Single Beam Bathymetry Data. Provided on Request* (Sydney, Australia).

Donatelli, C., Ganju, N. K., Zhang, X., Fagherazzi, S., and Leonardi, N. (2018). Salt Marsh Loss Affects Tides and the Sediment Budget in Shallow Bays. *J. Geophys. Res. Earth Surf.* 123, 2647–2662. doi: 10.1029/2018JF004617

Du, J., Shen, J., Zhang, Y. J., Ye, F., Liu, Z., Wang, Z., et al. (2018). Tidal Response to Sea-Level Rise in Different Types of Estuaries: The Importance of Length, Bathymetry, and Geometry. *Geophys. Res. Lett.* 45, 227–235. doi: 10.1002/2017GL075963

Fagherazzi, S., Kirwan, M. L., Mudd, S. M., Guntenspergen, G. R., Temmerman, S., D'Alpaos, A., et al. (2012). Numerical Models of Salt Marsh Evolution: Ecological, Geomorphic, and Climatic Factors. *Rev. Geophys.* 50, RG1002. doi: 10.1029/2011RG000359

Friedrichs, C. T., and Aubrey, D. G. (1988). Non-Linear Tidal Distortion in Shallow Well-Mixed Estuaries: A Synthesis. *Estuar. Coast. Shelf Sci.* 27, 521–545. doi: 10.1016/0272-7714(88)90082-0

Friedrichs, C. T., Aubrey, D. G., and Speer, P. E. (1990). Impacts of Relative Sea-Level Rise on Evolution of Shallow Estuaries. *Residual Curr. Long-term Transp.* 38, 105–122. doi: 10.1007/978-1-4613-9061-9_9

Ganju, N. K., Brush, M. J., Rashleigh, B., Aretxabaleta, A. L., del Barrio, P., Grear, J. S., et al. (2016). Progress and Challenges in Coupled Hydrodynamic-Ecological Estuarine Modeling. *Estuaries Coasts* 39, 311–332. doi: 10.1007/s12237-015-0011-y

Gedan, K. B., Kirwan, M. L., Wolanski, E., Barbier, E. B., and Silliman, B. R. (2011). The Present and Future Role of Coastal Wetland Vegetation in Protecting Shorelines: Answering Recent Challenges to the Paradigm. *Clim. Change* 106, (1), 7–29 doi: 10.1007/s10584-010-0003-7

Geoscience Australia. (2011). *LiDAR Elevation Data*. Available at: https://elevation.fsdf.org.au/ (Accessed 2.10.20).

Geoscience Australia. (2018). *LiDAR Elevation Data*. Available at: https://elevation.fsdf.org.au/ (Accessed 8.15.20).

Hagen, S. C., Morris, J. T., Bacopoulos, P., and Weishampel, J. F. (2013). Sea-Level Rise Impact on a Salt Marsh System of the Lower St. *Johns River. J. Waterw. Port Coastal Ocean Eng.* 139, 118–125. doi: 10.1061/(asce)ww.1943-5460.0000177

Haslett, S. K., Davies-Burrows, R., Panayotou, K., Jones, B. G., and Woodroff, C. D. (2010). Holocene Evolution of the Minnamurra River Estuary, Southeast Australia: Foraminiferal Evidence. *Z. Für Geomorphol.* 45, (3), 79–98. doi: 10.1127/0372-8854/2010/0054S3-0020

Hervouet, J.-M. (2000). TELEMAC Modelling System: An Overview. *Hydrol. Process* 14, 2209–2210. doi: 10.1002/1099-1085(200009)14:13<2209::AID-HYP23>3.0.CO;2-6

Hervouet, J.-M. (2007). *Hydrodynamics of Free Surface Flows: Modelling With the Finite Element Method, Hydrodynamics of Free Surface Flows: Modelling With the Finite Element Method* (Chichester, UK: John Wiley & Sons, Ltd). Available at: https://doi.org/10.1002/9780470319628.

Horstman, E. M., Bryan, K. R., and Mullarney, J. C. (2021). Drag Variations, Tidal Asymmetry and Tidal Range Changes in a Mangrove Creek System. *Earth Surf. Process. Landforms* 46 (9), esp.5124. doi: 10.1002/esp.5124

Horstman, E. M., Dohmen-Janssen, C. M., Bouma, T. J., and Hulscher, S. J. M. H. (2015). Tidal-Scale Flow Routing and Sedimentation in Mangrove Forests: Combining Field Data and Numerical Modelling. *Geomorph* 228, 244–262. doi: 10.1016/j.geomorph.2014.08.011

Iglesias, I., Avilez-Valente, P., Bio, A., and Bastos, L. (2019). Modelling the Main Hydrodynamic Patterns in Shallow Water Estuaries: The Minho Case Study. *Water* 11, 1–23. doi: 10.3390/w11051040

JCU Geophysics Laboratory. (2020). *Marotte HS-I User Guide*. Available at: https://www.marinegeophysics.com.au/current-meter/users-guide/.

Kaiser, G., Scheele, L., Kortenhaus, A., Løvholt, F., Römer, H., and Leschka, S. (2011). The Influence of Land Cover Roughness on the Results of High Resolution Tsunami Inundation Modeling. *Nat. Hazards Earth Syst. Sci.* 11, 2521–2540. doi: 10.5194/nhess-11-2521-2011

Kirwan, M. L., Guntenspergen, G. R., D'Alpaos, A., Morris, J. T., Mudd, S. M., and Temmerman, S. (2010). *Limits on the Adaptability of Coastal Marshes to Rising Sea Level* (n/a-n/a: Geophys. Res. Lett. 37). doi: 10.1029/2010GL045489

Kirwan, M. L., and Murray, A. B. (2007). A Coupled Geomorphic and Ecologic Model of Tidal Marsh Evolution. *Proc. Natl. Acad. Sci. U. S. A.* 104, (15), 6118–6122. doi: 10.1073/pnas.0700958104

Krauss, K. W., Mckee, K. L., Lovelock, C. E., Cahoon, D. R., Saintilan, N., Reef, R., et al. (2014). How Mangrove Forests Adjust to Rising Sea Level. *New Phytol.* 202, 19–34. doi: 10.1111/nph.12605

Krone, R. B. (1987). "A Method for Simulating Historic Marsh Elevations," in *Specialty Conference on Advances in Understanding of Coastal Sediment Processes*. Ed. N. C. Kraus (New Orleans: American Society of Civil Engineers), 316–322.

Kumbier, K., Carvalho, R. C., Vafeidis, A. T., and Woodroffe, C. D. (2018b). Investigating Compound Flooding in an Estuary Using Hydrodynamic Modelling: A Case Study From the Shoalhaven River, Australia. *Nat. Hazards Earth Syst. Sci.* 18, 463–477. doi: 10.5194/nhess-18-463-2018

Kumbier, K., Carvalho, R., and Woodroffe, C. (2018a). Modelling Hydrodynamic Impacts of Sea-Level Rise on Wave-Dominated Australian Estuaries With Differing Geomorphology. *J. Mar. Sci. Eng.* 6, 66. doi: 10.3390/jmse6020066

Kumbier, K., Hughes, M. G., Carvalho, R. C., and Woodroffe, C. D. (2022). Intertidal Wetland Geomorphology Influences Main Channel Hydrodynamics in a Mature Barrier Estuary. *Estuar. Coast. Shelf Sci.* 267, 107783. doi: 10.1016/j.ecss.2022.107783

Kumbier, K., Hughes, M. G., Rogers, K., and Woodroffe, C. D. (2021). Inundation Characteristics of Mangrove and Saltmarsh in Micro-Tidal Estuaries. *Estuar. Coast. Shelf Sci.* 261, 107553. doi: 10.1016/j.ecss.2021.107553

Lal, K. (2019). *Surface Elevation Dynamics Across a Range of Timescales in Coastal Wetlands of South-Eastern Australia. PhD Thesis* (Wollongong: University of Wollongong).

Lee, S. B., Li, M., and Zhang, F. (2017). Impact of Sea Level Rise on Tidal Range in Chesapeake and Delaware Bays. *J. Geophys. Res. Ocean.* 122, 3917–3938. doi: 10.1002/2016JC012597

Mazda, Y., Kanazawa, N., and Wolanski, E. (1995). Tidal Asymmetry in Mangrove Creeks. *Hydrobiologia* 295, 51–58. doi: 10.1007/BF00029110

Mazda, Y., Wolanski, E., King, B., Sase, A., Ohtsuka, D., and Magi, M. (1997). Drag Force Due to Vegetation in Mangrove Swamps. *Mangroves Saltmarshes* 1, 193–199. doi: 10.1023/A:1009949411068

McInnes, K., Church, J., Monselesan, D., Hunter, J., O'Grady, J., Haigh, I., et al. (2015). Information for Australian Impact and Adaptation Planning in Response to Sea-Level Rise. *Aust. Meteorol. Oceanogr. J.* 65, 127–149. doi: 10.22499/2.6501.009

McKee, K., Rogers, K., and Saintilan, N. (2012). Response of Salt Marsh and Mangrove Wetlands to Changes in Atmospheric CO2, Climate, and Sea Level, in: Global Change and the Function and Distribution of Wetlands. *Springer Netherlands Dordrecht* pp, 63–96. doi: 10.1007/978-94-007-4494-3_2

Mogensen, L. A., and Rogers, K. (2018). Validation and Comparison of a Model of the Effect of Sea-Level Rise on Coastal Wetlands. *Sci. Rep.* 8, 1–14. doi: 10.1038/s41598-018-19695-2

Morris, J. T., Sundareshwar, P. V., Nietch, C. T., Kjerfve, B., and Cahoon, D. R. (2002). Responses of Coastal Wetlands to Rising Sea Level. *Ecology* 83, 2869–2877. doi: 10.1890/0012-9658(2002)083[2869:ROCWTR]2.0.CO;2

Mudd, S. M., Howell, S. M., and Morris, J. T. (2009). Impact of Dynamic Feedbacks Between Sedimentation, Sea-Level Rise, and Biomass Production on Near-Surface Marsh Stratigraphy and Carbon Accumulation. *Estuar. Coast. Shelf Sci.* 82, 377–389. doi: 10.1016/j.ecss.2009.01.028

OEH. (2017). *Single Beam Bathymetry Data. Provided on Request* (Sydney, Australia).

Oliver, T. S. N., Rogers, K., Chafer, C. J., and Woodroffe, C. D. (2012). Measuring, Mapping and Modelling: An Integrated Approach to the Management of Mangrove and Saltmarsh in the Minnamurra River Estuary, Southeast Australia. *Wetl. Ecol. Manage.* 20, 353–371. doi: 10.1007/s11273-012-9258-2

Owers, C. J., Rogers, K., and Woodroffe, C. D. (2016). Identifying Spatial Variability and Complexity in Wetland Vegetation Using an Object-Based Approach. *Int. J. Remote Sens.* 37, 4296–4316. doi: 10.1080/01431161.2016.1211349

Panayotou, K., Woodroffe, C. D., Jones, B. G., Chenhall, B., McLean, E., and Heijnis, H. (2007). Patterns and Rates of Sedimentary Infill in the Minnamurra River Estuary, South-Eastern Australia. *J. Coast. Res.* (50), 688–692. doi: 10.2307/26481674

Rodríguez, J. F., Saco, P. M., Sandi, S., Saintilan, N., and Riccardi, G. (2017). Potential Increase in Coastal Wetland Vulnerability to Sea-Level Rise Suggested by Considering Hydrodynamic Attenuation Effects. *Nat. Commun.* 8, 1–12. doi: 10.1038/ncomms16094

Rogers, K., Kelleway, J. J., Saintilan, N., Megonigal, J. P., Adams, J. B., Holmquist, J. R., et al. (2019a). Wetland Carbon Storage Controlled by Millennial-Scale Variation in Relative Sea-Level Rise. *Nature* 567, 91–95. doi: 10.1038/s41586-019-0951-7

Rogers, K., Mogensen, L. A., Davies, P., Kelleway, J., Saintilan, N., and Withycombe, G. (2019b). Impacts and Adaptation Options for Estuarine Vegetation in a Large City. *Landsc. Urban Plan.* 182, 1–11. doi: 10.1016/j.landurbplan.2018.09.022

Rogers, K., and Saintilan, N. (2021). Processes Influencing Autocompaction Modulate Coastal Wetland Surface Elevation Adjustment With Sea-Level Rise. *Front. Mar. Sci.* 8, 694039. doi: 10.3389/fmars.2021.694039

Rogers, K., Saintilan, N., and Copeland, C. (2012). Modelling Wetland Surface Elevation Dynamics and its Application to Forecasting the Effects of Sea-Level Rise on Estuarine Wetlands. *Ecol. Modell.* 244, 148–157. doi: 10.1016/J.ECOLMODEL.2012.06.014

Roy, P. S., Williams, R. J., Jones, A. R., Yassini, I., Gibbs, P. J., Coates, B., et al. (2001). Structure and Function of South-East Australian Estuaries. *Estuar. Coast. Shelf Sci.* 53, 351–384. doi: 10.1006/ecss.2001.0796

Ryan, T. J. (1992). The Contemporary Hydrodynamics and Evolutionary Development of the Minnamurra Estuary, New South Wales. Honors Thesis (University of Wollongong), 1–93.

Saintilan, N., Khan, N. S., Ashe, E., Kelleway, J. J., Rogers, K., Woodroffe, C. D., et al. (2020). Thresholds of Mangrove Survival Under Rapid Sea Level Rise. *Science (80-.)* 368, 1118–1121. doi: 10.1126/science.aba2656

Saintilan, N., and Rogers, K. (2013). The Significance and Vulnerability of Australian Saltmarshes: Implications for Management in a Changing Climate. *Mar. Freshw. Res.* 64, (1), 66–79. doi: 10.1071/MF12212

Saintilan, N., Rogers, K., Kelleway, J. J., and Sloane, D. R. (2018). Climate Change Impacts on the Coastal Wetlands of Australia. *Wetlands* 39, 1–10. doi: 10.1007/s13157-018-1016-7

Saintilan, N., Wilson, N. C., Rogers, K., and Rajkaran, A. (2014). Mangrove Expansion and Salt Marsh Decline at Mangrove Poleward Limits. *Glob. Change Biol.* 20, 147–157. doi: 10.1111/gcb.12341

Seenath, A., Wilson, M., and Miller, K. (2016). Hydrodynamic Versus GIS Modelling for Coastal Flood Vulnerability Assessment: Which is Better for Guiding Coastal Management? *Ocean Coast. Manage.* 120, 99–109. doi: 10.1016/j.ocecoaman.2015.11.019

Silvestri, S., Defina, A., and Marani, M. (2005). Tidal Regime, Salinity and Salt Marsh Plant Zonation. *Estuar. Coast. Shelf Sci.* 62, 119–130. doi: 10.1016/j.ecss.2004.08.010

Spier, D., Gerum, H. L. N., Noernberg, M. A., and Lana, P. C. (2016). Flood Regime as a Driver of the Distribution of Mangrove and Salt Marsh Species in a Subtropical Estuary. *J. Mar. Syst.* 161, 11–25. doi: 10.1016/j.jmarsys.2016.05.004

Stark, J., Smolders, S., Meire, P., and Temmerman, S. (2017). Impact of Intertidal Area Characteristics on Estuarine Tidal Hydrodynamics: A Modelling Study for the Scheldt Estuary. *Estuar. Coast. Shelf Sci.* 198, 138–155. doi: 10.1016/J.ECSS.2017.09.004

Telemac2D. (2014). *Telemac2D User Manual V7p0*. Available at: http://www.opentelemac.org/index.php/manuals/viewcategory/13-telemac-2d (Accessed 5.11.21).

Temmerman, S., Bouma, T. J., Govers, G., Wang, Z. B., De Vries, M. B., and Herman, P. M. J. (2005). Impact of Vegetation on Flow Routing and Sedimentation Patterns: Three-Dimensional Modeling for a Tidal Marsh. *J. Geophys. Res. Earth Surf.* 110, 1–18. doi: 10.1029/2005JF000301

Temmerman, S., Bouma, T. J., Van de Koppel, J., van der Wal, D., De Vries, M. B., and Herman, P. M. J. (2007). Vegetation Causes Channel Erosion in a Tidal Landscape. *Geology* 35, 631. doi: 10.1130/G23502A.1

Temmerman, S., Govers, G., Meire, P., and Wartel, S. (2003a). Modelling Long-Term Tidal Marsh Growth Under Changing Tidal Conditions and Suspended Sediment Concentrations, Scheldt Estuary, Belgium. *Mar. Geol.* 193, 151–169. doi: 10.1016/S0025-3227(02)00642-4

Temmerman, S., Govers, G., Wartel, S., and Meire, P. (2003b). Spatial and Temporal Factors Controlling Short-Term Sedimentation in a Salt and

Freshwater Tidal Marsh, Scheldt Estuary, Belgium, SW Netherlands. *Earth Surf. Process. Landforms* 28, 739–755. doi: 10.1002/esp.495

Thorne, K., MacDonald, G., Guntenspergen, G., Ambrose, R., Buffington, K., Dugger, B., et al. (2018). U.S. Pacific Coastal Wetland Resilience and Vulnerability to Sea-Level Rise. *Sci. Adv.* 4, 1–10. doi: 10.1126/sciadv.aao3270

University of New South Wales. (2017). *LiDAR Elevation Data. Provided on Request* (Sydney, Australia).

Watson, J. G. (1928). Mangrove Forests of the Malay Peninsula. *Malayan For. Rec.* 6, 1–275.

Wiberg, P. L., Fagherazzi, S., and Kirwan, M. L. (2020). Improving Predictions of Salt Marsh Evolution Through Better Integration of Data and Models. *Ann. Rev. Mar. Sci.* 12, 389–413. doi: 10.1146/annurev-marine-010419-010610

Williams, J. J., and Esteves, L. S. (2017). Guidance on Setup, Calibration, and Validation of Hydrodynamic, Wave, and Sediment Models for Shelf Seas and Estuaries. *Adv. Civ. Eng.* 2017, 1–26. doi: 10.1155/2017/5251902

Woodroffe, C. D. (2018). Mangrove Response to Sea Level Rise: Palaeoecological Insights From Macrotidal Systems in Northern Australia. *Mar. Freshw. Res.* 69, 917–932. doi: 10.1071/MF17252

Woodroffe, C. D., Rogers, K., McKee, K. L., Lovelock, C. E., Mendelssohn, I. A., and Saintilan, N. (2016). Mangrove Sedimentation and Response to Relative Sea-Level Rise. *Ann. Rev. Mar. Sci.* 8, 243–266. doi: 10.1002/andp.18341081502

Zhang, X., Church, J. A., Monselesan, D., and McInnes, K. L. (2017). Sea Level Projections for the Australian Region in the 21st Century. *Geophys. Res. Lett.* 44, 8481–8491. doi: 10.1002/2017GL074176

Conflict of Interest: The authors declare that the research was conducted in the absence of any commercial or financial relationships that could be construed as a potential conflict of interest.

Publisher's Note: All claims expressed in this article are solely those of the authors and do not necessarily represent those of their affiliated organizations, or those of the publisher, the editors and the reviewers. Any product that may be evaluated in this article, or claim that may be made by its manufacturer, is not guaranteed or endorsed by the publisher.